

Studies on Molecular Basis for FOXO1-DNA Damage Responses

January 2016

Yuta KANEKO

Studies on Molecular Basis for FOXO1-DNA Damage Responses

A Dissertation Submitted to

The Graduate School of Life and Environmental Sciences,

The University of Tsukuba

In Partial Fulfillment of the Requirements

For the Degree of Doctor of Philosophy in Agricultural Science

(Doctoral Program in Life Sciences and Bioengineering)

Yuta KANEKO

Contents

| | | |
|---------------------|--|-----------|
| Chapter I. | Preface | 1 |
| Chapter II. | FOXO1/DAF-16 is a functional component required for translesion DNA synthesis | |
| | Summary | 3 |
| | Introduction | 4 |
| | Materials and Methods | 7 |
| | Results | 13 |
| | Discussion | 20 |
| Chapter III. | CTF18 interacts with RPA complex in Response to Replication stresses | |
| | Summary | 34 |
| | Introduction | 36 |
| | Materials and Methods | 39 |
| | Results | 42 |
| | Discussion | 46 |
| Chapter IV. | Concluding Remarks | 55 |
| | Acknowledgments | 57 |
| | References | 58 |

Chapter 1

Preface

Genomic DNA is constantly exposed to endogenous and exogenous genotoxic insults that introduce DNA damage and cause the not only mutation but also direct interference with DNA replication and transcription. Therefore, all of the organisms conserve a variety of DNA damage response for maintenance of genome integrity, and the disruption is thought to be a possible cause of carcinogenesis, aging and developmental abnormality (1,2). In particular, replication stress response that is the protective mechanism against defects in chromosome replication is highly regulated by a series of transducer proteins for maintaining genome integrity in eukaryotic cells. The forkhead box O (FOXO) family of transcription factors play crucial role in diverse biological processes, orchestrating programs of gene expression that regulate stress resistance, tumor suppression and development (3). In mammals, FOXO family consists of four members, FOXO1, FOXO3, FOXO4, and FOXO6, while invertebrates have only one FOXO gene, such as *dFOXO* in the *Drosophila* and *daf-16* in the *Caenorhabditis elegans*. FOXO proteins are tightly regulated by multiple posttranslational modifications, including phosphorylation, acetylation, ubiquitination and arginine methylation. (4,5) Among them, a major form of regulation is Akt-mediated phosphorylation downstream of insulin or IGF-1 signaling pathways and that results in the export of FOXO proteins from the nucleus to the cytoplasm, thereby repressing the

transcription of FOXO target genes. Genetic studies in *C. elegans* have revealed that reduction-of-function mutations of *daf-2*, an ortholog of the mammalian insulin/IGF-1 receptor, extend lifespan up to three fold, and this extension is entirely dependent on *daf-16* (6) (7). As mention above, although accumulating evidences indicates that FOXO contributes to anti-aging, tumor suppression and development, which likely to be closely related to genomic stability, the involvement of FOXO/DAF-16 in DNA damage response remains largely unknown. In this study, I focused on the two themes to get deep insight into the function of FOXO1 on DNA damage response during DNA synthetic phase. First, I investigated the involvement of FOXO1 in translesion DNA synthesis, which is error-free bypass against UV-induced replication arrest, and suggested that FOXO1/DAF-16 is required for s-phase UV tolerance in both mammalian cells and *c. elegans* (Chapter II). Through this study, I found that FOXO1 interacts with RPA complex, which is platform protein in DNA damage response. Second, I verified that the interaction between CTF18-RFC and RPA complex, two of which are essential components for s-phase DNA damage response to get deep insight into the not only the genome stability during s-phase but also the relationship between FOXO1 and DNA damage response (Chapter III).

Chapter II

FOXO1/DAF-16 is a functional component required for translesion DNA synthesis

Summary

Forkhead box O (FOXO; DAF-16 in nematode) transcription factors activate a program of genes that control stress resistance, metabolism, and lifespan. Given the adverse impact of the stochastic DNA damage on organismal development and ageing, we examined the role of FOXO/DAF-16 in UV-induced DNA-damage response. Knockdown of FOXO1, but not FOXO3a, increases sensitivity to UV irradiation when exposed during S phase, suggesting a contribution of FOXO1 to translesion DNA synthesis (TLS), a replicative bypass of UV-induced DNA lesions. Actually, FOXO1 depletion results in a sustained activation of the ATR-Chk1 signaling and a reduction of PCNA monoubiquitination following UV irradiation. FOXO1 does not alter the expression of TLS-related genes but binds to the protein replication protein A (RPA1) that coats single-stranded DNA and acts as a scaffold for TLS. In *Caenorhabditis elegans*, *daf-16* null mutants show UV-induced retardation in larval development and are rescued by overexpressing DAF-16 mutant lacking transactivation domain, but not substitution mutant unable to interact with RPA-1. Thus, our findings demonstrate that FOXO1/DAF-16 is a functional component in TLS independently of its transactivation activity.

Introduction

The forkhead box O (FOXO) family of transcription factors play crucial role in diverse biological processes, orchestrating programs of gene expression that regulate cell-cycle progression, metabolism and stress resistance. In mammals, FOXO family consists of four members, FOXO1, FOXO3, FOXO4, and FOXO6, while invertebrates have only one FOXO gene, such as *dFOXO* in the *Drosophila* and *daf-16* in the *Caenorhabditis elegans*. FOXO proteins are tightly regulated by multiple posttranslational modifications, including phosphorylation, acetylation, ubiquitination and arginine methylation (8,9). Among them, a major form of regulation is Akt-mediated phosphorylation downstream of insulin or IGF-1 signaling pathways and that results in the export of FOXO proteins from the nucleus to the cytoplasm, thereby repressing the transcription of FOXO target genes. Genetic studies in *C. elegans* have revealed that reduction-of-function mutations of *daf-2*, an ortholog of the mammalian insulin/IGF-1 receptor, extend lifespan up to three fold, and this extension is entirely dependent on *daf-16* (10). Accordingly, gene expression regulated by DAF-16 is considered to be a trigger for promoting anti-ageing and longevity, and to date a number of approaches have identified various DAF-16 target genes that controls detoxification, lipolysis and autophagy. Meanwhile, although accumulating evidence indicates that ageing is accompanied by an increase in genomic instability, the involvement of FOXO/DAF-16 in DNA damage response remains largely unknown.

Among the numerous harmful agents, ultraviolet (UV) irradiation is a ubiquitous environmental stress, which generates two types of DNA lesions, cyclobutane pyrimidine dimers (CPDs) and (6-4) photoproducts (11). These UV-induced DNA lesions are usually removed by one of the most versatile DNA repair systems called nucleotide excision repair (NER), whereas if left unrepaired until S phase, they interfere with the progress of replication forks catalyzed by DNA polymerases. In order to prevent the collapse of stalled replication forks, which in turn leads to DNA double-strand breaks, translesion DNA synthesis (TLS) is performed by the Y-family DNA polymerases, including Pol η , Pol κ , Pol ι and Rev1(12). When replication forks block at CPD sites, Pol η has been shown to replace the stalled replicative DNA polymerases depending on monoubiquitination of the clamp protein, proliferating cell nuclear antigen (PCNA), by the E3 ubiquitin ligase RAD18(13). This modification is activated by single-stranded DNA (ssDNA) coated with the ssDNA binding protein, Replication Protein A (RPA), whereby monoubiquitinated PCNA has an increased affinity for Pol η , thus helping to recruit Pol η to stalled replication forks and allowing accurate replicative bypass of CPD by incorporating correct bases on the opposite strand. Together with PCNA, the clamp loader replication factor C (RFC) complex, and RPA have been shown to stimulate the DNA synthetic activity of Pol η (14-16). On the other hand, defects in Pol η result in a cancer-prone and UV-sensitive inherited syndrome, a variant form of xeroderma pigmentosum, suggesting that Pol η is essential for preventing UV-induced skin cancers (17).

Previously, our laboratory found that knockdown of FOXO1, but not FOXO3a, increases sensitivity to UV specifically when irradiated during S phase in mammalian cells. In addition, FOXO1 depletion also abrogates the progression of S phase after UV irradiation and thereby inhibits cell proliferation. These results led me to hypothesize that FOXO1 would be implicated in the TLS process.

Here, I tested whether FOXO1/DAF-16 is involved in TLS. Supporting my hypothesis, knockdown of FOXO1 results in a sustained activation of the ATR-Chk1 pathway and a reduction of PCNA monoubiquitination. FOXO1 does not alter the expression of TLS-related genes, but it binds to RPA1 through the forkhead domain and this binding enables FOXO1 to target an ssDNA *in vitro*. In addition, I find that FOXO/DAF-16 plays a key role in the UV-induced DNA damage tolerance in nematodes. Compared to wild-type controls, *daf-16* null mutants showed UV-induced delay in larval development, while UV irradiation has no effect on adult lifespan, suggesting that DAF-16 confers UV tolerance only during somatic cell proliferation in *C. elegans*. Furthermore, rescue experiments revealed that transactivation function of DAF-16 is not necessary for the UV tolerance in larval development. Taken together, my findings demonstrate an evolutionally conserved and transactivation-independent FOXO1/DAF-16 function in the UV-induced DNA damage tolerance that may contribute, at least in part, to genomic stability by preventing stalled replication forks from degenerating into deleterious DNA structures.

Materials and methods

Cell culture, transfection and siRNA

HEK293, HEK293T, HeLa and MCF7 cells were cultured in DMEM supplemented with 10%FBS. Plasmid transfection was performed using GeneJuice Transfection Reagent (Novagen) according to the manufacture's protocol. siRNA duplexes were synthesized by Nippon EGT and transfected using Lipofectamine RNAiMAX (Invotrogen). The siRNA sequences are described below;

human FOXO1 (#1: 5'-AGUUCAUUCGUGUGCAGAATT-3',

#2: 5'-AGAGCUGCAUCCAUGGACATT-3'),

Polh (5'-GUGGAGCAGCGGCAAAAUCTT-3'),

FOXO3a (5'- GAGCTCTTGGTGGATCATC-3'),

GADD45a (5-GGAUCCUGCCUUAAGUCAACUUAUU -3'),

luciferase (5'-UAAGGCUAUGAAGAGAUACTT-3').

The following siRNAs were purchased: Rad18 (SANTA CRUZ, sc-72142),

Control siRNA against GFP (B-Bridge, S10C-0300)

(5'-CUACAACAGCCACAACGUC-3')

Plasmid construction and antibodies

Full-length cDNAs encoding human Polh, CTF18, PCNA, RPA1, RPA2, RPA3, RAD18, and *C. elegans rpa-1* were amplified by PCR and then cloned into either pcDNA3-FLAG, pcDNA3-HA, pEGFP-C1, pVenus-N1 or pGEX-6P vectors.

Expression vectors for mouse FOXO1, FOXO3a, and *C. elegans daf-16* were described previously. Deletion mutants of RPA1 were generated by PCR and then inserted into pGEX-5X vector. The GP (W193G/H199P) and DAD (lacking 473-510 a.a.) mutants of *daf-16* were generated by PCR and then inserted into pPD95_81 vector. The following antibodies were purchased: anti-HA (3F10) from Roche; anti-CTF18 (A301-883A) from BETHYL; anti-Polh (ab17725), anti-RPA1 (ab79398), anti-RPA2 (ab2175), anti-RAD18 (ab57447) from abcam; anti-PCNA (610664), anti-ORC2 (51-6875GR) from BD; anti-b-actin (A5316) from Sigma Aldrich; anti-Chk1 (K0086-3), anti-FLAG (M185-3L), anti-cyclobutane pyrimidine dimmers (CPD), anti-(6-4) photoproducts (6-4PPs) from Medical & biological laboratories; anti-GFP (#2956), anti-FOXO1 (#2880), anti-FOXO3a (#2497), anti-phospho-Chk1 (Ser345) (#2341), anti-ATM (#2873), anti-phospho-ATM (Ser1981) (#5883) from Cell Signaling Technology; anti-H2AX(#07-627), anti-gH2AX (05-636) from Merck Millipore; GADD45a (sc-797) from SANTACRUZ.

Cell synchronization

Cell cycle synchronization was performed as reported previously (18). Briefly, HEK293 cells were synchronized at the G1/S transition by double thymidine block. For S-phase synchronization, cells were released from the second block for the indicated times.

Co-immunoprecipitation

Co-immunoprecipitation was performed as previously described. Briefly, whole-cell lysate from HEK293 cells were immunoprecipitated with normal IgG or anti-FOXO1 antibody, followed by Western blotting with antibodies as indicated.

GFP-Pol η foci formation

HEK293 cells were sequentially transfected with 20 nM siRNA and GFP-Pol η and then irradiated with UV (20 J/m²). After 6 h, cells were fixed with 3.7% formalin/PBS for 10 min at room temperature and stained with Hoechst 33258. At least 100 nuclei were observed by fluorescent microscopy and nuclei containing more than twenty bright foci were scored as positive.

Generation of transgenic lines

Extrachromosomal arrays carrying transgenic strains were generated using standard microinjection methods. For rescue of *daf-16(mu86)* mutants, genomic DNA fragments containing 4,029 bp of 5' flanking sequence and either wild-type (*daf-16WT(+)*), GP mutant (*daf-16GP(+)*) or DAD mutant (*daf-16DAD (+)*) of *daf-16a1* were ligated to the pPD95_81 vector and injected at 100 ng ml⁻¹ with *Pmyo-2::DsRed* at 5 ng ml⁻¹ into CF1038: *daf-16(mu86)I*. The extrachromosomal array was integrated by UV irradiation and then outcrossed to *daf-16(mu86)I* three times.

Luciferase assay

Luciferase assays were performed as described. Briefly, HEK293T cells were seeded in 24-well plate and transfected with indicated plasmids. pCMV-b-galactosidase plasmid was included to control for efficiency of transfection and empty plasmid was added to ensure equal DNA amounts in each transfection. The luciferase activity was measured with a Wallac 1420 multilabel counter (PerkinElmer) and normalized for b-galactosidase activity in the same sample.

GST pull-down assay

GST fusion proteins were expressed in *E. coli* strain BL-21 by using the pGEX vector system. Various GST-fused proteins immobilized on glutathione-Sepharose were incubated with cell extracts from transfected HEK293T cells or *in vitro* translated protein (TnT system, Promega), which was diluted with binding buffer (50 mM Hepes, pH7.9/ 150 mM NaCl/ 0.1% TritonX-100/ protease inhibitors). After incubation for 4 h at 4°C, the beads were washed three times with the same buffer, and proteins were analyzed by Western blotting.

Single-stranded DNA pull-down assay

ssDNA pull-down assay was performed as described (19) with some modifications.

| | | |
|---|--------|-----------------|
| Biotinylated | 50-mer | oligonucleotide |
| (TTGTAAAACGCGGCCAGTGAATTCATCATCAATATTCCTTTTTTGGCAGGCG | | |

G TGTTAATACTGCCGCC) was bound to streptavidin-beads (Dynal) according to the manufacturer's directions, and then incubated with the purified FLAG-RPA proteins in 500 μ l of binding buffer (50 mM Tris-HCl (pH7.5)/ 150 mM NaCl/ 0.1% TritonX-100) at 4 °C for 30 min. The beads were retrieved, washed three times with binding buffer, and incubated with cell lysate expressing HA-FOXO1 or HA-FOXO3a proteins together with poly-(dI-dC) (20 μ g/ml) at 4 °C for 1 h. The beads were retrieved and washed with binding buffer, followed by Western blotting.

***C. elegans* strains**

All strains were cultured according to standard methods. Strains used were Bristol N2 wild-type, CF1038 *daf-16(mu86)I*, XF656 *polh-1(ok3317)III*, RB864 *xpa-1(ok698)I*, TJ356 *zIs356[daf-16::GFP;rol-6]*, TKB222 *trcIs22[daf-16WT::GFP];daf-16(mu86)I*, TKB230 *trcIs18[daf-16GP::GFP];daf-16(mu86)I*, TKB231 *trcIs24[daf-16DAD::GFP];daf-16(mu86)I*.

Larval development assay

Synchronized L1 larvae (about 50 worms) were exposed to UV (20 J/m²) on NGM plates without OP50 and then transferred to NGM plates with OP50. The number of larvae at each stage was counted at post-irradiation periods when over 80% of the non-irradiated L1 larvae of each strain developed to the L4 stage.

Adult lifespan assay

Life span assays were conducted at 20 °C. Synchronized L1 larvae (about 100 worms) were grown to young adult and then transferred to plates without OP50. Following UV irradiation at 20 J/m², worms were transferred back to OP50-seeded NGM plates containing floxuridine (0.5 mg /ml) for preventing progeny production. Animals were tapped every day and scored as dead when they did not respond to the platinum wire pick. All of the life span assays were repeated at least two times.

Cellular localization analysis of DAF-16::GFP in L1 larvae

Synchronized L1 larvae of TJ356 were grown on NGM plates with OP50 for 4 h at 20 °C, and then washed off the plates with M9 buffer and transferred to NGM plates without OP50. Following UV irradiation at 20 J/m², the worms were grown for 3 h on NGM plates with OP50 and then observed under the fluorescence microscope.

Results

FOXO1 knockdown promotes a sustained activation of the ATR-Chk1 signaling after UV irradiation.

Because defects in TLS results in stalled replication forks at CPD sites and then ATR phosphorylates/activates the effector kinase Chk1, I tested the possible involvement of FOXO1 in TLS by measuring ATR-induced phosphorylation of Chk1 at serine-345. HEK293 cells transfected with control or FOXO1 siRNA were synchronized in early S phase followed by exposure to UV, and then further incubated for 2, 6 or 9 hr. As shown in Figure II-1A, knockdown of FOXO1 led to a marked increase in the phosphorylation levels of Chk1 at 2 hr post-UV, and also caused a subsequent sustained Chk1 phosphorylation until 9 hr post-UV even when the phospho-Chk1 signals completely disappeared in control cells. It should be noted that, consistent with previous report (20), Pol η knockdown cells show the similar increased and sustained phosphorylation of Chk1 following UV irradiation (Figure II-1B). In contrast, Chk1 hyperphosphorylation by knockdown of FOXO1 or Pol η was not observed neither when cells were irradiated with UV in G₁ phase nor when cell proliferation was blocked by pretreatment with hydroxyurea (HU) (Figure II-1C and D). Collectively, these findings suggest that FOXO1 depletion results in sustained activation of ATR-signaling in response to UV-induced replication block, probably due to defects in TLS.

Unlike FOXO1, knockdown of FOXO3a failed to alter the phosphorylation levels of Chk1 (Figure II-1E). On the other hand, FOXO3a has been reported to promote

autophosphorylation/activation of ataxia telangiectasia mutated (ATM) by direct interaction and thus activate its downstream mediators to control damage-induced cell-cycle checkpoints and DNA repair (21). This result suggests that, in contrast to FOXO3a, FOXO1 could regulate ATR-signaling downstream of UV-damage response.

FOXO1 is partially required for PCNA monoubiquitination but not for Pol η foci formation.

Since PCNA monoubiquitination triggers a switching from the replicative polymerase blocked at a lesion to Pol η , I first studied the effects of FOXO1 depletion on PCNA monoubiquitination. HEK293 cells transfected with control or FOXO1 siRNA were synchronized in early S phase followed by exposure to 20 J/m² UV, and 2, 4 or 6 hr later, chromatin fraction and whole cell lysates were analyzed by Western blot. As shown in Figure II-2A, knockdown of FOXO1 resulted in a slight but significant decrease in monoubiquitination level of PCNA at all periods after UV irradiation. Furthermore, the amount of RAD18 proteins in chromatin fraction was also diminished by FOXO1 depletion, suggesting that UV-induced RAD18 loading is influenced by FOXO1 (Figure II-2B).

In order to further examine the involvement of FOXO1 in TLS, I next focused on subcellular translocation of Pol η after exposure to UV (22). I observed that transiently expressed GFP-Pol η was localized uniformly in the nucleus of control knockdown cells at basal state and actually accumulated into nuclear foci following UV irradiation (Figure II-2C and D). The foci formation was markedly abolished by knockdown of

RAD18, whereas FOXO1 depletion had no effect on the UV-induced assembly of Pol η foci (Figure II-2C and D). Taken together, these results indicate that FOXO1 is partially required for at least PCNA monoubiquitination, but not for the Pol η foci formation in the initiation of TLS.

FOXO1 does not regulate the expression of TLS-related genes but binds to RPA1.

To clarify the molecular mechanism underlying the contribution of FOXO1 to TLS pathway, I first tested the possibility that FOXO1 may regulate gene expression of Pol η and its related proteins, such as the clamp protein PCNA, the clamp loader complex CTF18-RFC, and the ssDNA-binding protein RPA, all of which have been shown to stimulate the DNA synthetic activity of Pol η (15,16). However, neither knockdown of FOXO1 nor transfection of constitutively active FOXO1 (3A), where all three Akt phosphorylation sites are substituted with alanine, alter the expression levels of Pol η , CTF18, PCNA, RPA1, RPA2, and RAD18 in HEK293 cells (Figure II-3A and B). These results indicate that the contribution of FOXO1 to TLS appears not to be dependent on the expression of TLS-related genes.

Instead, given the physical interaction of FOXO3a with ATM as mentioned above (21), I investigated whether FOXO1 could form a complex with TLS machinery including Pol η , PCNA, RPA1 and CTF18. Co-immunoprecipitation assay showed that endogenous FOXO1 binds specifically to RPA1 in HEK293 cells (Figure II-3C). Because RPA1 is a subunit of RPA heterotrimeric complex together with RPA2 and RPA3 (23), I attempted to determine which components bind to FOXO1 by preparing

bacterially expressed GST-FOXO1 and whole cell lysates expressing Venus-RPA1, -RPA2, and -RPA3 proteins. GST pull-down assays demonstrated that FOXO1 preferentially binds to RPA1 *in vitro* (Figure II-3D).

Forkhead domain of FOXO1 is required for RPA1 binding.

Furthermore, I constructed a series of deletion mutants of FOXO1 and found that the forkhead DNA-binding domain is responsible for interacting with RPA1 (Figure II-4A). To confirm this result, I generated FOXO1 (GP) mutant harboring two point substitution (W206G and H212P) that impairs the structure of forkhead domain and thereby results in a significant reduction of DNA-binding activity (24). As shown in Figure II-4B and C, GP mutation completely abolished the FOXO1-RPA1 interaction *in vitro* and *in vivo*. Meanwhile, I identified the C-terminus of RPA1 called DBD-C as a binding region for FOXO1 (Figure II-4D). RPA is known to not only bind and stabilize ssDNA regions during DNA replication and repair, but also recruit a variety of DNA processing proteins through direct interaction (23). Therefore, I tested whether FOXO1 could be recruited to ssDNA region through interaction with RPA1. I found that FOXO1 fails to directly bind to ssDNA, whereas addition of RPA1 enables FOXO1 to bind to ssDNA in a dose-dependent manner, indicating that recruitment of FOXO1 to ssDNA is entirely dependent on the presence of RPA1 (Figure II-4F). In addition, although FOXO3a also bound to RPA1-ssDNA, this interaction was relatively low in comparison with FOXO1 (Figure II-4F). Taken together, these results suggest that RPA1 could be a candidate scaffold protein for FOXO1 to participate in TLS process.

FOXO/DAF-16 is required for UV tolerance during larval development in *C. elegans*.

The possible involvement of FOXO1 in TLS led us next to determine whether this function could be conserved across species. A genetic study with the nematode *Caenorhabditis elegans* (*C. elegans*) is often used for evaluating the functions of the FOXO ortholog DAF-16 and actually providing evidence that several longevity pathways converge on DAF-16 (25). In this study, since TLS is accompanied with DNA replication, I focused on *C. elegans* larvae whose somatic tissues are composed of proliferative cells, and sought to assess the effect of UV-induced DNA damage on the progression of larval development from L1 to L4 (Figure II-5A). First, to address whether DAF-16 responds to UV irradiation during L1 stage, I observed cellular localization of DAF-16::GFP *in vivo* (26). Although DAF-16::GFP was normally localized in the cytoplasm without UV, I found a predominant nuclear localization after exposure to 20 J/m² UV in L1 larvae (Figure II-5B). Next, wild-type N2, the *daf-16* null-mutant *daf-16(mu86)* and a null mutant for the *C. elegans* ortholog of *polh*, *polh-1(ok3317)* were synchronized to L1 larvae and immediately exposed to 20 J/m² UV. Thereafter, when over 80% of each control (no UV) animal reached to the L4 larvae, the developmental stages of UV-irradiated animals were distinguished into L1/L2, L3 and L4 stages. I found that UV irradiation causes a substantial and an almost complete arrest of larval development in *daf-16(mu86)* and *polh-1(ok3317)* mutants, respectively, while only a slight retardation was observed in N2 (Figure II-5C). These

results suggest that DAF-16 contributes to UV-induced DNA damage tolerance in larval development, albeit with lower contribution compared to POLH-1.

Since, unlike larval stages, the somatic tissues in the adulthood are quiescent and composed of post-mitotic cells, UV sensitivity of adult *C. elegans* was predicted not to be dependent on TLS process. To test this hypothesis, I evaluated UV-resistance of N2, *daf-16(mu86)* and *polh-1(ok3317)* together with *xpa-1(ok698)*, a loss-of-function mutant in the NER pathway, from one-day-old adult with or without UV irradiation. As expected, I found that N2, *daf-16(mu86)* and *polh-1(ok3317)* mutants exhibit no significant difference in the survival curves between UV-irradiated and unirradiated animals (Figure II-5D-F). Importantly, consistent with a previous report (27), *xpa-1(ok698)* mutants were highly sensitive to UV during adulthood, likely due to the lack of NER (Figure II-5G). Collectively, these results suggest that DAF-16 as well as POLH-1 plays a critical role in TLS, but not NER in *C. elegans*.

FOXO/DAF-16 contributes to UV tolerance during larval development independently of its transactivation function.

Finally, to explore which functions of DAF-16 are required for the UV tolerance during larval development, I attempted to perform rescue experiments with transgenic lines expressing wild-type or two mutants of *daf-16*; GP and DAD, in *daf-16(mu86)* background. The DAF-16 GP mutant harbors point mutations at the conserved tryptophan (W) and histidine (H) residues within the forkhead DNA-binding domain (corresponding to FOXO1 GP), while the DAF-16 DAD mutant lacks the C-terminus

(residues 473-510) primarily responsible for transactivation function (28) (Figure II-6A).

I first confirmed that DAF-16 GP, but not DAD mutant, is indeed unable to interact with RPA-1, the *C. elegans* ortholog of RPA1 (Figure II-6B). In addition, luciferase assay using the two DAF-16 mutants demonstrated that both of them fail to induce the transcriptional activity of a reporter construct (Figure II-6C). Thereafter, I generated three integrated lines, *trcIs35[daf-16wt(+):gfp];daf-16(mu86)*,

trcIs36[daf-16DAD(+):gfp];daf-16(mu86) and

trcIs18[daf-16GP(+):gfp];daf-16(mu86) and examined the effect of UV-induced DNA damage on the progression of larval development. As shown in Figure II-6D, transgenic rescue with *daf-16WT* entirely restored the progression of larval development of *daf-16(mu86)* mutants after UV irradiation. Most importantly, a similar improvement was also observed in *Is36[daf-16DAD(+):gfp];daf-16(mu86)* animals, whereas *daf-16GP* failed to rescue the decreased UV tolerance in *daf-16(mu86)* background.

Taken together, these data indicate that DAF-16-dependent UV tolerance in larval development requires not the transactivation function of DAF-16, but the forkhead domain as an interaction region with RPA-1.

Discussion

In the current study, I demonstrate that FOXO1 has a role in translesion DNA synthesis in addition to its known role as a transcription factor. FOXO1 contributes to the UV damage response when specifically irradiated during S-phase and is partially required for UV-inducible RAD18 loading, PCNA monoubiquitination, but not for Pol η foci formation (17). Accordingly, knockdown of FOXO1 results in the sustained activation of the ATR-Chk1 signaling after UV irradiation, probably due to defects in TLS. Moreover, FOXO1 is able to bind to a single-stranded DNA by interacting with RPA1 through the forkhead domain. In *C. elegans*, DAF-16/FOXO plays a key role in the UV-induced DNA damage tolerance during larval development. Importantly, rescue experiments with functional mutants of DAF-16 revealed that the forkhead domain responsible for RPA-1-binding, but not transactivation domain, could be necessary for the UV tolerance ability of DAF-16/FOXO.

My present results imply that FOXO1/DAF-16 contributes to TLS following UV irradiation independently of its transactivation function. How does FOXO1/DAF-16 influence UV tolerance during DNA replication? Interestingly, several reports have established chromatin remodeling as a new regulatory process in relatively early step of TLS. For example, in yeast, two distinct chromatin-remodeling complexes, INO80 and RSC, promote RAD18 recruitment at stalled replication forks, thereby facilitating PCNA ubiquitination and TLS. Additionally, in mammals, transcriptional repressor ZBTB1 has shown to control KAP-1-dependent chromatin remodeling to promote

UV-inducible PCNA monoubiquitination during TLS (29,30). Given my findings that FOXO1 knockdown reduced PCNA monoubiquitination (Figure II-2A and B), FOXO1/DAF-16 could be involved in recruiting a chromatin-remodeling complex through interacting with ssDNA-bound RPA1 to stalled replication forks. Supporting this idea, a recent study has reported that DAF-16 employs the chromatin remodeler SWI/SNF as cofactors to regulate its target genes and increases stress resistance and longevity, even though there is no evidence that SWI/SNF also serve as chromatin remodeler in TLS (31). Instead, it should be noted that FOXO1 itself is known to be able to disrupt core histone:DNA contacts and open compacted chromatin arrays in the IGFBP-1 promoter (32), raising the possibility that the chromatin opening ability of FOXO1 is solely sufficient to facilitate TLS. Further studies are needed to elucidate the relationship between FOXO1/DAF-16-mediated UV tolerance and chromatin remodeling.

My findings from biochemical and transgenic rescue experiments argue that FOXO1/DAF-16 contributes to DNA damage tolerance by forming a complex with RPA1 through the forkhead domain and also propose a model in which transcription factor FOXO1/DAF-16 participates in an inherent function of RPA, namely binding and stabilizing of ssDNA regions during TLS. In contrast, a recent study has demonstrated that RPA1 helps recruitment of transcription factor HSF1 to nucleosomal DNA by recruiting histone chaperone FACT and thus enables constitutive HSF1 access to nucleosomal DNA for both basal and inducible gene expression (33). Taken together, these results provide the possibility that RPA1 and transcription factors mutually affect

and regulate each other's function, including DNA repair, DNA replication and transcription. Indeed, since RPA1 strongly represses the transcriptional activity of FOXO1 (data not shown), presumably through masking the forkhead DNA-binding domain, RPA1 interaction may be a trigger for switching of FOXO1 function from transcriptional activation to DNA damage tolerance.

FOXO1 has been shown to undergo post-translational modifications, including phosphorylation, acetylation, ubiquitination, lysine and arginine methylation, and glycosylation, those of which can regulate transactivation function of FOXO1 by modulating the subcellular localization, protein stability, DNA-binding, transcriptional activity, and interaction with other proteins (4,5,34). In addition, our laboratory previously reported that Poly(ADP-ribose)polymerase-1 (PARP1) binds and poly(ADP-ribosyl)ates FOXO1 (35); however, the functional significance of poly(ADP-ribosyl)ation remains unclear. It is well-established that, following DNA damage, PARP1 senses and binds to DNA single and double strand breaks, whereby it becomes activated and thus catalyzes the attachment of poly(ADP)ribose polymers onto substrates, including transcription factors, histones, and PARP1 itself (36). Besides opening chromatin, poly(ADP)ribosylation causes PARP1 dissociation from DNA, allowing for access to an orchestrated network of repair enzymes involved in the base-excision repair, nucleotide-excision repair, mismatch repair, and DNA double-strand break repair. In particular, a recent study reported that PARP10, a mono-ADP-ribosyl transferase, interacts with PCNA and is required for DNA damage tolerance(37). Although the relationship between FOXO1 and PARP10 in TLS is

unknown, these findings together with my results here suggest a possible involvement of PARP activity in FOXO1/DAF-16-mediated UV tolerance.

Here, I provide evidence that impaired function of FOXO1 results in sustained activation of the ATR-Chk1 axis after UV irradiation during S-phase (Figure II-1A). On the other hand, consistent with previous report (21), our laboratory found that FOXO3a promotes autophosphorylation of ATM and thus phosphorylates downstream H2AX even when irradiated with UV (data not shown). These results demonstrate that although FOXO1 and FOXO3a appear to have both distinct and overlapping functions that could be compensated with each other, there is a functional difference in transactivation-independent DNA-damage responses. In addition, considering that ATR disruption leads to early embryonic lethality unlike ATM-null mice (38,39), my findings may provide an explanation for a distinct phenotype of two FOXO knockout mice; FoxO1-null mice die at embryonic day 10.5, while FoxO3-null mice are viable and have no apparent phenotype (40).

In *C. elegans*, *daf-16* as well as *polh-1* is required for UV tolerance during larval development, but not during adulthood (Figure II-5). These different resistance patterns among stages could be attributed to whether the somatic cells proliferate when irradiated with UV. Since lifespan is typically defined as the number of days after the adult molt and in which *C. elegans* consists only of post-mitotic cells, with the exception of germline precursor cells, it seems likely that DAF-16-mediated longevity occurs independently of its TLS function. In support of this idea, Polh-deficient mice are viable and do not show any obvious spontaneous defects, such as premature

ageing-like phenotype, at least during the first year of life (41). Alternatively, given that these mutant mice are highly susceptible to developing skin carcinomas following chronic exposure to UV irradiation, FOXO1-mediated UV tolerance may also play a role in decreasing the risk of genomic instability by preventing stalled replication forks from degenerating into defective DNA structures.

Recently, Mueller *et al.* reported that DAF-16 alleviates DNA-damage-induced developmental arrest and promotes developmental growth even in the absence of nucleotide excision repair (42). They argue that DAF-16 is activated in response to persistent DNA damage and induces somatic growth genes through binding to the GATA transcription factor EGL-27 whose Zinc finger domain in turn recognizes the consensus sequence overlapping the GATA and the DAF-16-associated element (DAE) in the target gene promoter. Most importantly, however, the developmental growth especially when overriding persistent DNA lesions requires TLS and our present findings provide a mechanism whereby DAF-16 binds to RPA1 and facilitates TLS without transcriptional activation. Thus, these dual functions of DAF-16 would cooperatively play a critical role in UV tolerance during larval development.

In conclusion, here I present evidence that FOXO1/DAF-16 contributes to UV-induced DNA damage tolerance independently of its transcriptional activity in mammalian cells and *C. elegans*. This conserved mechanism was not relevant to longevity in *C. elegans*, but alternatively, may be involved in other FOXO functions, in particular, such as stem cell maintenance in mammals (43,44). If so, in view of the notion that aberrant stem cell function is a hallmark of ageing (2), our findings will

provide new insights into the molecular mechanism of ageing and the pathogenesis of age-related diseases, including type 2 diabetes, Alzheimer's disease and cancer.

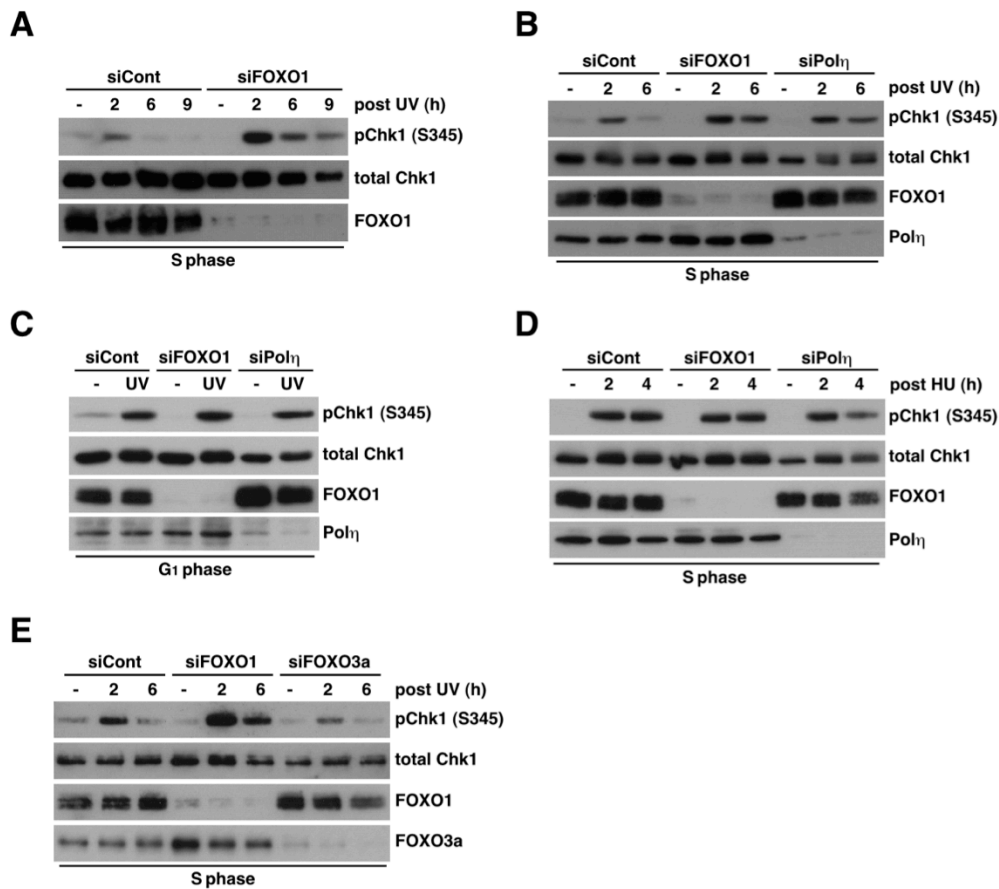


Figure II-1 Knockdown of FOXO1 promotes a sustained phosphorylation of Chk1 after UV irradiation.

(A and B) Silencing FOXO1 or Polh results in enhanced and sustained phosphorylation of Chk1 after UV irradiation during S phase. HEK293 cells transfected with indicated siRNAs were synchronized at S phase. After exposure to UV (20 J/m^2), whole-cell lysates were immunoblotted with antibodies as indicated. (C) Silencing FOXO1 or Polh has no effects on phosphorylation of Chk1 after UV irradiation during G₁ phase. HEK293 cells transfected with indicated siRNAs were synchronized at G₁ phase, treated with or without UV (20 J/m^2), and after 6 hr, whole-cell lysates were immunoblotted with antibodies as indicated. (D) Silencing FOXO1 has no effect on phosphorylation of Chk1 after treatment with hydroxyurea (HU, 1 mM) during S phase. HEK293 cells transfected with indicated siRNAs were synchronized at S phase. After treatment with HU, whole-cell lysates were immunoblotted with antibodies as indicated. (E) Silencing FOXO3a has no effect on phosphorylation of Chk1 after UV irradiation during S phase.

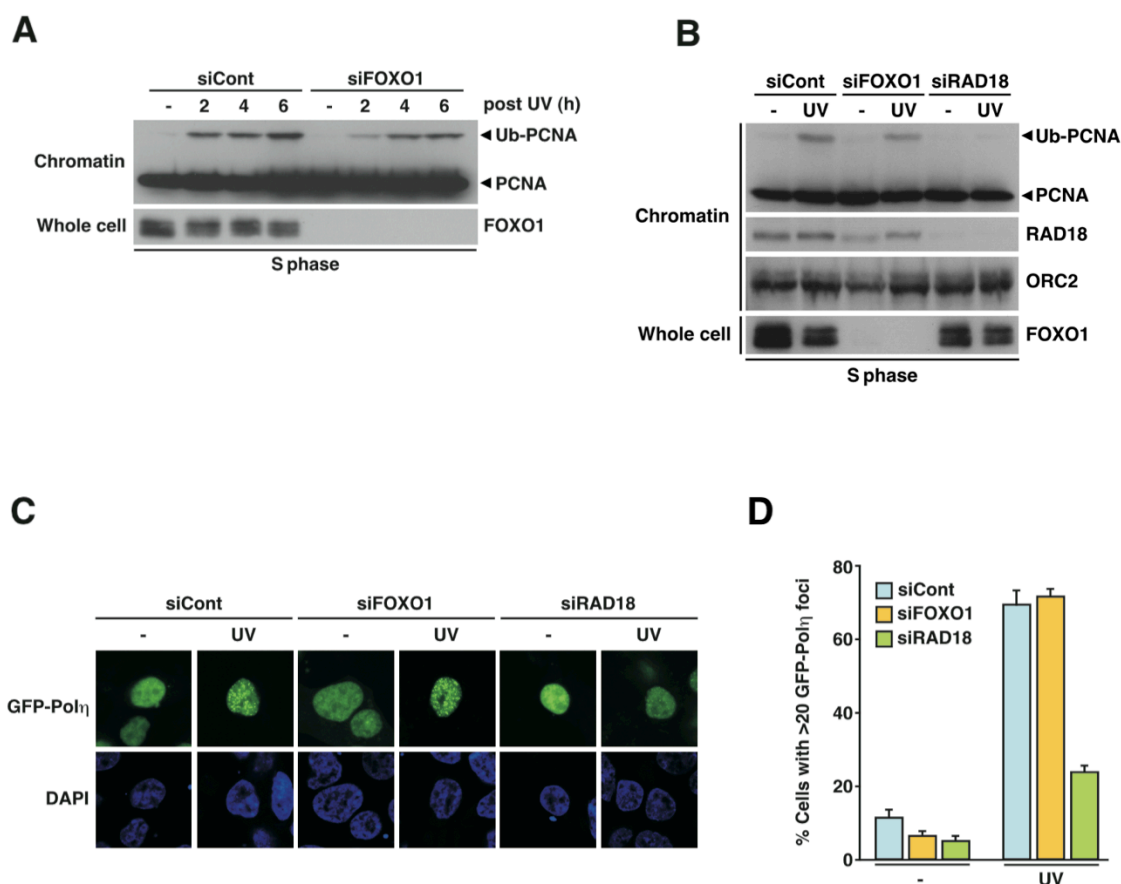


Figure II-2 FOXO1 is required for PCNA monoubiquitination, but not for Polh foci formation.

(A) FOXO1 is partially responsible for UV-inducible PCNA monoubiquitination. HEK293 cells were transfected with indicated siRNAs, treated with or without UV (20 J/m²), and after 2, 4, and 6 hr, chromatin fractions and whole-cell lysates were immunoblotted with antibodies as indicated.

(B) HEK293 cells were transfected with indicated siRNAs, treated with or without UV (20 J/m²), and after 6 hr, chromatin fractions and whole-cell lysates were immunoblotted with antibodies as indicated. (C) FOXO1 is not required for UV-inducible foci formation of Polh. HEK293 cells were sequentially transfected with indicated siRNAs and GFP-Polh, treated with or without UV (20 J/m²), and after 6 hr, fixed and observed by fluorescent microscopy. (D) Quantification of cells displaying more than twenty GFP-Polh foci in (C).

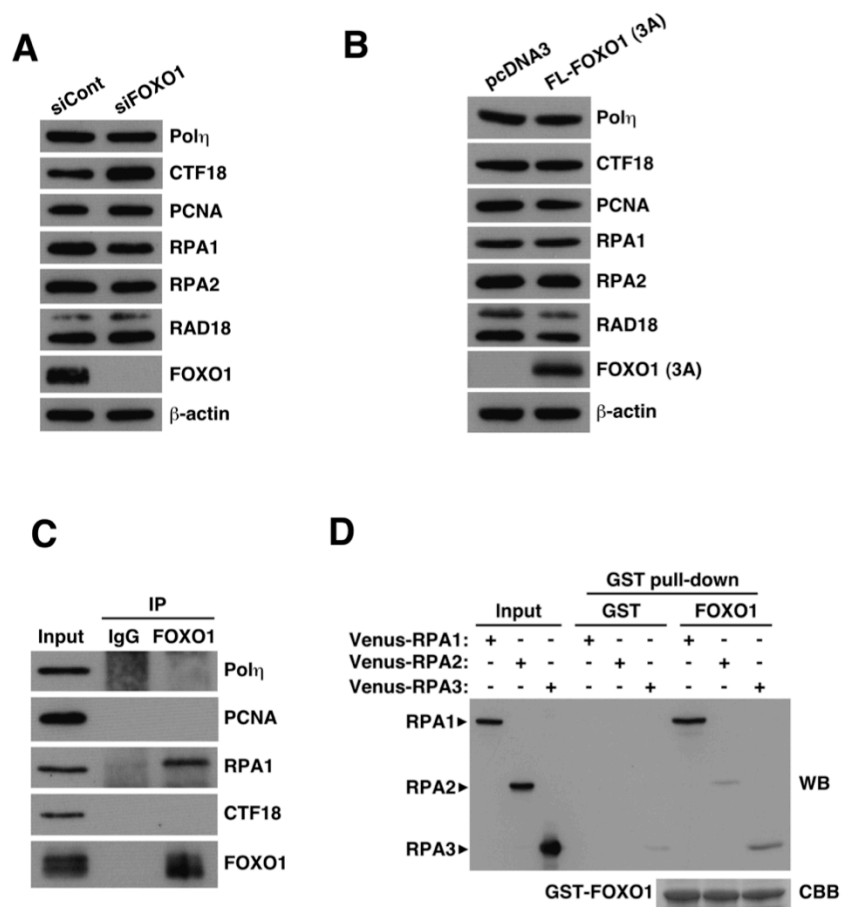
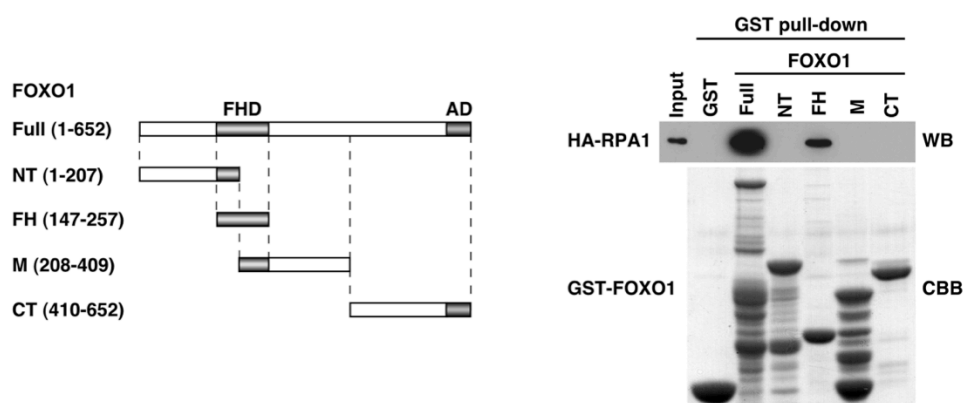


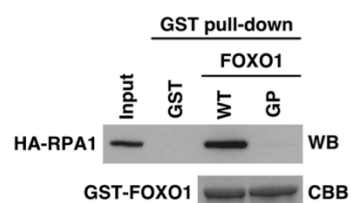
Figure II-3 FOXO1 is not involved in TLS-related genes expression, but binds to RPA1

(A) FOXO1 does not regulate the expression of TLS-related genes. Whole-cell lysates from HEK293 cells transfected with control or FOXO1 siRNA were immunoblotted with antibodies as indicated. (B) Whole-cell lysates from HEK293T cells transfected with empty or FOXO1 (3A) expression plasmid were immunoblotted with antibodies as indicated. (C) Endogenous FOXO1 interacts with RPA1. Whole-cell lysates from HEK293 cells were immunoprecipitated with normal IgG or anti-FOXO1 antibody, followed by Western blotting with antibodies as indicated. (D) FOXO1 specifically interacts with RPA1 *in vitro*. Whole-cell lysates from HEK293T cells expressing Venus-RPA1, -RPA2 or -RPA3 were incubated with GST or GST-FOXO1, followed by Western blotting with anti-Venus antibody. GST proteins are shown by CBB staining.

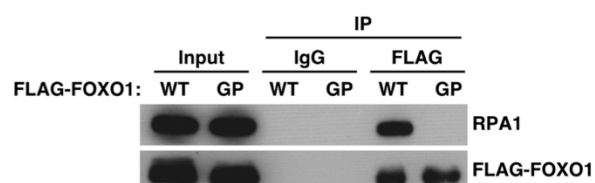
A



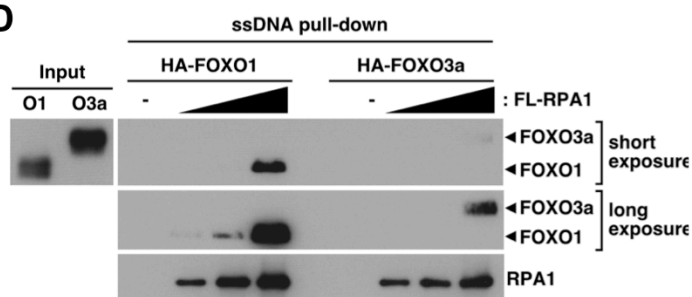
B



C



D



E

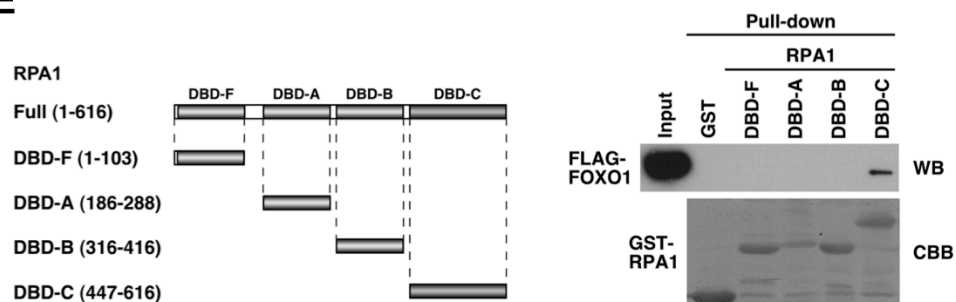


Figure II-4 Forkhead domain of FOXO1 is required for RPA1 binding.

(A) Forkhead domain of FOXO1 is required for RPA1 binding. (Left) Schematic of FOXO1 deletions. FHD, forkhead domain; AD, activation domain (Right) Whole-cell lysates from HEK293T cells expressing HA-RPA1 were incubated with GST or a series of GST-FOXO1 deletions, followed by Western blotting with anti-HA antibody. GST proteins are shown by CBB staining. (B) FOXO1 (GP) mutation abolishes the interaction with RPA1. Whole-cell lysates from HEK293T cells expressing HA-RPA1 were incubated with GST, GST-FOXO1 wild-type or GP mutant, followed by Western blotting with anti-HA antibody. GST proteins are shown by CBB staining. (C) FOXO1 (GP) mutant fails to bind to RPA1. Whole-cell lysates from HEK293T cells expressing FLAG-FOXO1 wild-type or GP mutant were immunoprecipitated with normal IgG or anti-FLAG antibody, followed by Western blotting with antibodies as indicated. (D) FOXO1 is recruited to ssDNA in a manner dependent on RPA1. ssDNA-conjugated beads were preincubated with increasing amounts of FLAG-RPA1, and then incubated with whole-cell lysates from HEK293T cells expressing HA-FOXO1 or -FOXO3a, followed by Western blotting with indicated antibodies. (E) DBD-C domain of RPA1 is required for FOXO1 binding. (Left) Schematic of RPA1 deletions. DBD, DNA-binding domain (Right) Whole-cell lysates from HEK293T cells expressing FLAG-FOXO1 were incubated with GST or a series of GST-RPA1 deletions, followed by Western blotting with anti-FLAG antibody. GST proteins are shown by CBB staining.

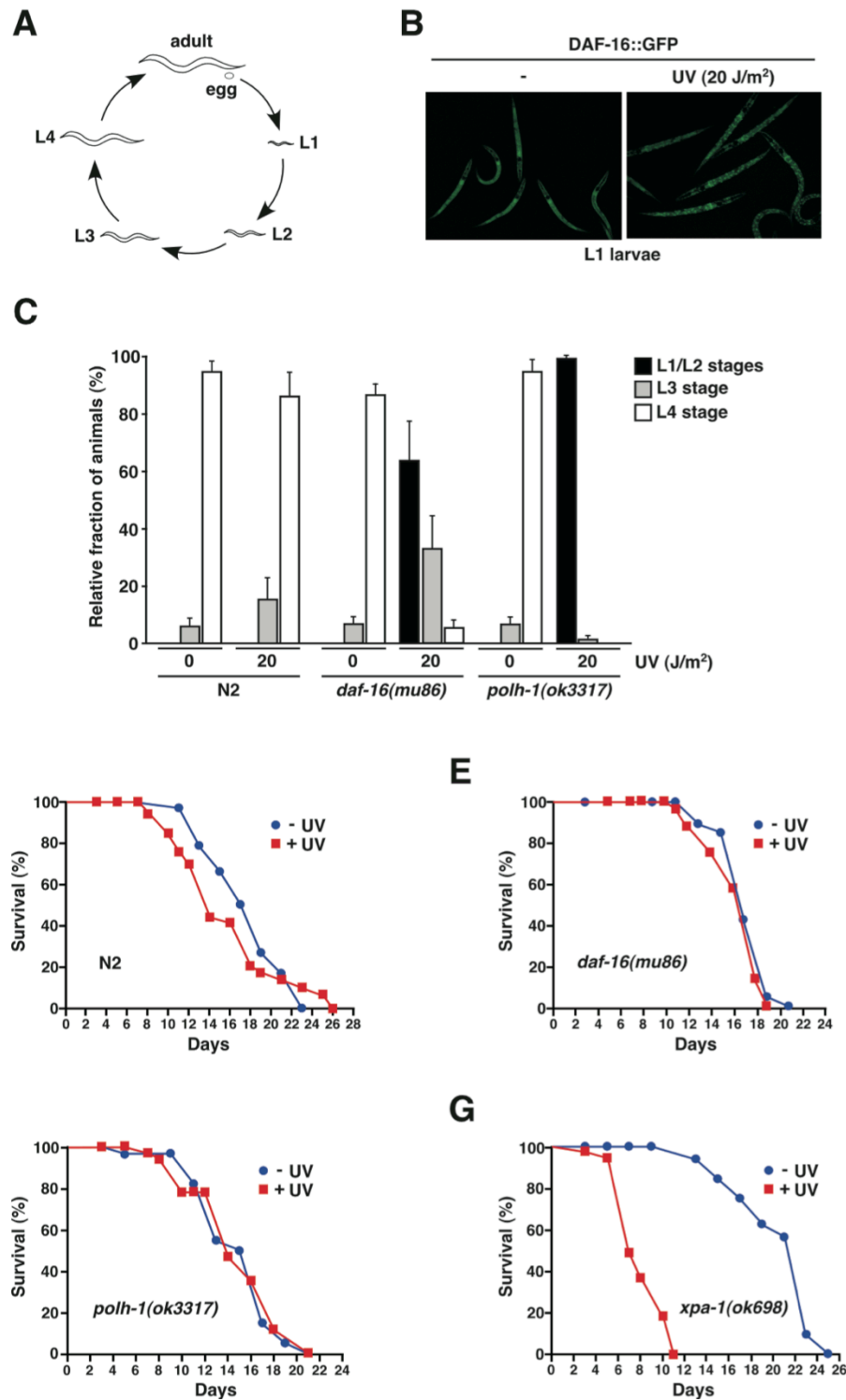


Figure II-5 DAF-16 contributes to UV tolerance during larval development but not adult lifespan in *C. elegans*.

(A) Schematic of the life cycle of *C. elegans*. *C. elegans* passes through four larval stages (L1-L4) to reach adulthood. (B) GFP::DAF-16 accumulates in the nucleus after exposure to UV during L1 larvae. Synchronized L1 larvae of TJ356 strain were exposed to UV (20 J/m²), and after 3 hr, observed by fluorescent microscopy. (C) Effects of UV irradiation on larval development of N2, *daf-16* and *polh-1* mutants. Synchronized L1 larvae were exposed to UV (20 J/m²) and when over 80% of each control (no UV irradiation) animal developed to the L4 larvae, the developmental stages of UV-irradiated animals were counted as each of L1/L2, L3 and L4 stages. (D-G) Effects of UV irradiation on adult lifespan. Survival of N2, *daf-16*, *polh-1* and *xpa-1* mutants were measured with or without UV irradiation (50 J/m²).

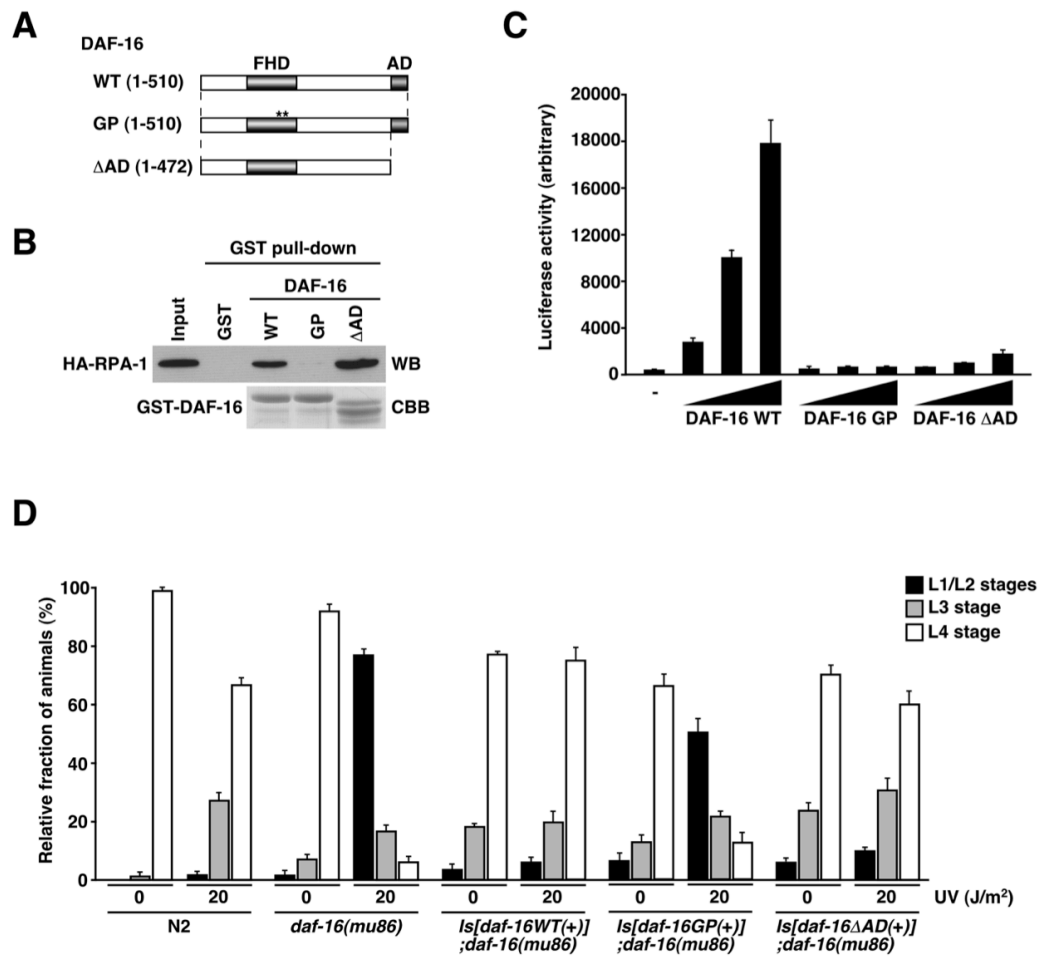


Figure II-6 Transactivation function of DAF-16 is not required for UV tolerance during larval development.

(A) Schematic of DAF-16 mutants. FHD, forkhead domain; AD, activation domain; GP, W193G/H199P. (B) DAF-16 GP but not DAD mutant fails to bind to *C. elegans* RPA-1. In vitro translated HA-RPA1 was incubated with GST, GST-FOXO1 wild-type, GP, or DAD mutant, followed by Western blotting with anti-HA antibody. GST proteins are shown by CBB staining. (C) Both DAF-16 GP and DAD fail to transactivate the reporter gene. HEK293T cells were transfected with luciferase reporter construct (3xIRS-MLP-luc) together with increasing amounts of DAF-16 wild-type, GP, or DAD as indicated. After 48 h, luciferase activities were measured and presented as arbitrary units. Values are shown as mean \pm s.d. ($n = 3$). (D) Effects of UV irradiation on larval development of transgenic animals. Synchronized L1 larvae were exposed to UV (20 J/m²) and when over 80% of each control (no UV irradiation) animal developed to the L4 larvae, the developmental stages of UV-irradiated animals were counted as each of L1/L2, L3 and L4 stages.

Chapter III

CTF18 interacts with RPA complex in response to Replication stresses

Summary

Replication stress response is a protective mechanism against defects in chromosome replication for maintaining genome integrity in eukaryotic cells. Clamp protein PCNA and clamp loader replication factor C (RFC), core component of the replication machinery, function as not only processivity factor of DNA replication but also a scaffold for replication-associated events. An alternative clamp loader complex called CTF18-RFC has been shown to act as a positive regulator of the two types of replication stress response: the S-phase checkpoint signaling and the translesion DNA synthesis. However, it remains largely unknown how CTF18-RFC responds to replication stress and is recruited to stalled replication forks. Here, I show that endogenous CTF18 forms a physical complex with a single-stranded DNA-binding protein RPA, which acts as a scaffold for DNA processing proteins, in mammalian cells. By using an *in situ* proximity ligation assay (PLA), we found that the interaction of CTF18 with RPA occurs in chromatin by replication stress such as hydroxyurea and UV irradiation, which triggers s-phase checkpoint response and translesion DNA synthesis. Furthermore, the PLA demonstrated that the kinetics of the interaction between CTF18 and RPA correlate positively with that of Chk1 phosphorylation, which is an indicator of activation of the S-phase checkpoint signaling. Given dynamic changes of

chromosome during replication and DNA damage response, kinetic analyses are important for the investigation into replication stress response. These findings provide new insights into the molecular mechanism whereby CTF18-RFC participates in the regulation of replication stress response.

Introduction

Chromosome replication is a risky process for maintaining genome integrity, because if DNA lesions exist during DNA synthesis, they interfere with the progress of replication forks and thereby result in an excessive formation of single-strand DNA (ssDNA) that could be a major cause of deleterious lesions, such as DNA double-strand breaks (45,46). To preserve genome integrity during chromosome replication, eukaryotic cells have acquired several adaptive mechanisms of DNA damage response (1,2). One of the most studied pathways is the S-phase checkpoint response, which is evoked by an exposure of ssDNA at stalled replication forks, resulting from the consequences of defects in DNA synthesis and the progression of the DNA helicase. The checkpoint kinase ATR (ATM and Rad3-related) is recruited on ssDNA where newly coated with ssDNA-binding protein, Replication Protein A (RPA), and then causes the phosphorylation and activation of downstream checkpoint kinase Chk1, which in turn leads to the maintenance of fork stability for preserving genome integrity (19,47,48). Another is a damage tolerance mechanism called the translesion DNA synthesis, the major process with which cells replicate past the unrepaired DNA lesion during S phase (12). When replication forks are blocked at DNA lesions, such as UV-induced cyclobutane pyrimidine dimers (CPDs), the Y-family DNA polymerases Pol η replaces the stalled replicative DNA polymerases depending on monoubiquitination of the ring-shaped clamp protein, proliferating cell nuclear antigen (PCNA), by the E3 ubiquitin ligase RAD18 (12). Monoubiquitinated PCNA has an

increased affinity for Pol η , thus helping to recruit to stalled replication forks and allowing accurate replicative bypass of CPD by incorporating correct bases on the opposite strand (22,49). Consequently, TLS overcomes UV-induced replication blocks, thereby preventing sustained activation of the S-phase checkpoint in response to an excessive formation of ssDNA (50).

Accumulating evidence has shown that the S-phase checkpoint and the translesion DNA synthesis are both activated by conserved clamp loader complex called CTF18-RFC (Ctf: Chromosome Transmission Fidelity; RFC: Replication Factor C) (15,51-54). CTF18-RFC is one of the four “heteropentameric RFC complexes” each of which contains a common small subunit comprising RFC2–4 together with a unique largest subunit, including either RFC1, Elg1, RAD17, or CTF18. RFC1-RFC plays an important role in normal DNA replication by serving to load the homotrimeric PCNA clamp around the junction of primers with template DNA at replication forks (55). Elg1-RFC is involved in the maintenance of genome stability (56,57), while RAD17-RFC contributes to activate the DNA damage checkpoint by loading the heterotrimeric 9-1-1 checkpoint clamp at sites of damaged DNA (58). Meanwhile, although CTF18-RFC was originally reported to play an important role in the establishment of sister chromatid cohesion, recent studies with budding yeast have shown that CTF18-RFC mediates activation of the S-phase checkpoint depending on the association with DNA polymerase epsilon (59). In contrast, a biochemical study with *in vitro* reconstitution system has demonstrated that CTF18-RFC binds to and stimulates the DNA synthetic activity of DNA polymerase eta (15). However, the

molecular mechanisms underlying these alternative functions of CTF18-RFC remain largely unknown.

Materials and methods

Cell culture, transfection

HEK293 cells were kept at 37°C in humidified 5% CO₂ atmosphere and cultured in Dulbecco's modified Eagle's medium (nacalai tesque) supplemented with 10% fetal bovine serum and 100 U penicillin/streptomycin (Sigma-Aldrich). Plasmid transfection was performed using GeneJuice Transfection Reagent (Novagen) according to the manufacture's protocol.

Plasmid construction and antibodies

Full-length cDNAs encoding human CTF18, RPA1, RPA2 and RPA3 were amplified by PCR and then cloned into either pcDNA3-FLAG, pcDNA3-HA, pEGFP-C1 or pGEX-6P vectors. Deletion mutants of RPA1 were generated by PCR and then inserted into pGEX-5X vector. The following antibodies were purchased: anti-HA (3F10) from Roche; anti-CTF18 (A301-883A) from BETHYL; anti-RPA1 (ab79398), anti-RPA2 (ab2175), from abcam.

Cell synchronization

Cell cycle synchronization was performed by the double thymidine block method as reported previously (60). Briefly, exponentially growing HEK293 cells were treated with 2 mM thymidine for 16 hours, thymidine-free media for 10 hours, and 2 mM thymidine for 18 hours to arrest the cell cycle at the G1/S boundary. Then, cells were released in fresh medium and analyzed at various time intervals.

Co-immunoprecipitation

Co-immunoprecipitation was performed as previously described. Briefly, whole-cell lysate from HEK293 cells were immunoprecipitated with normal IgG or anti-CTF18 antibody, followed by Western blotting with antibodies as indicated.

GST pull-down assay

GST fusion proteins were expressed in *E. coli* strain BL-21 by using the pGEX vector system. Various GST-fused proteins immobilized on glutathione-Sepharose were incubated with *in vitro* translated protein (TnT system, Promega), which was diluted with binding buffer (50 mM Hepes, pH7.9/ 150 mM NaCl/ 0.1% TritonX-100/ protease inhibitors). After incubation for 2 h at 4°C, the beads were washed three times with the same buffer, and proteins were analyzed by Western blotting.

Single-stranded DNA pull-down assay

ssDNA pull-down assay was performed as described (19) with some modifications.

| | | |
|---|--------|-----------------|
| Biotinylated | 50-mer | oligonucleotide |
| (TTGTAAAACGCGGCCAGTGAATTCATCATCAATATTCCTTTTTTGGCAGGCG | | |
| G TGTTAATACTGCCGCC) | | |

was bound to streptavidin-beads (Dynal) according to the manufacturer's directions, and then incubated with the purified FLAG-RPA proteins in 500 µl of binding buffer (50 mM Tris-HCl (pH7.5)/ 150 mM NaCl/ 0.1% TritonX-100) at 4 °C for 30 min. The beads were retrieved, washed three times with binding buffer,

and incubated with cell lysate expressing HA-CTF18 proteins together with poly-(dI-dC) (20 µg/ml) at 4 °C for 1 h. The beads were retrieved and washed with binding buffer, followed by Western blotting.

In situ Proximity ligation assay (PLA)

PLA was performed according to the manufacturer's instructions. Briefly, synchronized HEK293 cells at S phase were treated with hydroxyurea or UV light, and then extracted with CSK buffer (10 mM PIPES-NaOH, pH 6.8, 300 mM sucrose, 100 mM NaCl) containing 0.5% Triton X-100 for 5 minutes for detection of chromatin bound proteins (61). After washing with CSK buffer without Triton X-100, cells were fixed with 3.7% formalin for 20 minutes, followed by permeabilization with ice-cold methanol for 10 min. After blocking with Duolink Blocking solution, cells were probed with both mouse monoclonal anti-RPA2 and rabbit polyclonal anti-CTF18 antibodies. All fluorescence data were obtained with a confocal microscope FV10i (OLYMPUS) and z-stacked images (collected in 1 µm steps) were used for quantification of PLA signals with Duolink Image Tool (Sigma-Aldrich).

Result

CTF18 interacts with RPA complex in vivo and in vitro.

To elucidate the mechanism underlying replication stress responses by CTF18-RFC, I attempted to identify a new binding partner of CTF18 and focused on an ssDNA-binding protein RPA that acts as a scaffold for DNA processing proteins. Since RPA is a heterotrimeric complex composed of 70, 32, and 14 kDa subunits (referred to as RPA1, RPA2, and RPA3, respectively) (23), I examined a possible interaction between CTF18 and each RPA subunits with co-immunoprecipitation assay. As shown in Figure III-1A, endogenous levels of CTF18 bound to RPA1 and RPA2 in HEK293 cells. To further investigate whether these interactions occur directly, GST pull-down assays were performed by using bacterially expressed GST-RPAs and *in vitro* translated CTF18 proteins. Due to the failure of preparing full-length GST-RPA1 as soluble fusion proteins, RPA1 was divided into four fragments based on the conserved functional domains, DBD-F, DBD-A, DBD-C, and DBD-C (Figure III-1B)(23). Unlike the result from co-immunoprecipitation, CTF18 did not interact with RPA2, but bound preferentially to DBD-A domain of RPA1, which is responsible for the initial interaction with ssDNA (Figure III-1C). Next, I tested whether CTF18 could be recruited to ssDNA through the interaction with RPA1 by using ssDNA pull-down assays. Beads-conjugated single-strand oligonucleotides were preincubated with or without an increasing amount of the FLAG-RPA1 proteins and after washing, these samples were further incubated with HA-CTF18 proteins. While CTF18 alone failed to bind to ssDNA *in vitro*, addition of RPA1 enabled CTF18 to bind to ssDNA in a

dose-dependent manner (Figure III-1D). Taken together, these data suggest that CTF18 can form a physical complex with RPAs on ssDNA.

CTF18 is associated with RPA in presence of replication stress.

If the interaction between CTF18 and RPA occurs in the process of replication stress response, it was expected that the CTF18-RPA complexes could be observed in the nucleus when replication forks are stalled during S-phase. To test this possibility, I used the DuoLink *in situ* proximity ligation assay (PLA), in which two endogenous proteins are immunostained with different species-specific secondary antibodies that are linked to complementary oligonucleotides. In this assay, when two distinct antibodies locate in close proximity, the linked DNA can be amplified and visualized with a fluorescent probe as foci that represent molecules of each of two interacting proteins. To induce the S-phase checkpoint response, double-thymidine arrested HEK293 cells were released into S-phase and then treated with hydroxyurea (HU), which causes a reversible inhibition of DNA synthesis and thus blocks the progression of replication forks. As shown in Figure III-2A, no significant signal was detected in the absence of HU. In contrast, HU treatment resulted in the formation of PLA foci in the nucleus in a dose-dependent manner (Figure III-2A and B). These results suggest that S-phase checkpoint response elicited by stalled replication forks leads to the interaction between CTF18 and RPA in the nucleus.

CTF18 interacts with RPA after UV-irradiation.

In addition to the S-phase checkpoint pathway, eukaryotic cells can tolerate replication stress by bypassing DNA lesions through the translesion DNA synthesis (12). Since CTF18 has been also implicated in the translesion DNA synthesis (15), I investigated whether UV-induced DNA damage could become a trigger of the CTF18-RPA interaction during S phase. Synchronized HEK293 cells at S phase were exposed to UV irradiation at 20 or 100 J/m², and after 2 h, the CTF18-RPA interaction was assessed by counting PLA foci. I observed a few foci in the nucleus after an exposure to 20 J/m² UV and this foci formation was substantially augmented when irradiated with 100 J/m² UV (Figure III-3A and B). Although it is not possible to exclude that S-phase checkpoint response also occurs by UV irradiation, these results raise the possibility that CTF18 binds to RPA in the process of translesion DNA synthesis.

PLA signals between CTF18 and RPA gradually decrease with time course.

Finally, I examined the dissociation kinetics of CTF18-RPA complex by tracking the time course of PLA signals after UV-induced replication stress. I found that while the number of foci peaks at 2 h after UV irradiation, it gradually decreases with time and almost disappears until 10 h (Figure III-4A and B). Considering that this time-dependent change in UV-induced binding of CTF18 to RPA is similar to that of Chk1 phosphorylation at Ser345 (Figure III-4C), these data imply that the CTF18-RPA

interaction is actually correlated with the dynamics of replication stress response, particularly in translesion DNA synthesis.

Discussion

My data establish that CTF18, an alternative subunit of the RFC clamp loader, is a new binding partner of RPA in mammalian cells. I found that this interaction is triggered when replication stress occurs and then gradually diminished in accordance with a decrease in the phosphorylation levels of Chk1 at Ser345. Accumulating evidence has shown that CTF18-RFC complex plays critical roles in activation of the S-phase checkpoint and translesion DNA synthesis by interacting with DNA polymerase epsilon and eta, respectively (15,51-53). However, the mechanism whereby CTF18-RFC responds to replication stress and targets to stalled replication forks remains elusive. In this study, I present a hypothesis that RPA may serve as a platform for the molecular assembly of CTF18-RFC together with DNA polymerase epsilon and eta, which in turn helps an efficient response to replication stress.

The *in situ* proximity ligation assay demonstrated that replication stress induced by HU treatment or UV irradiation is a trigger of the interaction between CTF18 and RPA in the nucleus. These data raise the question of how CTF18 senses replication stress and binds preferentially to RPA on ssDNA. A possible mechanism could be the phosphorylation of RPA2 subunit in response to replication stress. Actually, several studies have shown that stalled replication forks strongly cause hyperphosphorylation of RPA2 at the N-terminal region through the DNA damage response pathways involving the ATR and the DNA-dependent protein kinase (DNA-PK) (61-64). Moreover, it is

noted that phosphorylation of RPA2 is known to prevent its association with the replication machinery and thus be considered as a trigger for redirecting RPA functions from DNA replication to DNA damage responses (23,64,65). In agreement with this idea, RPA2 phosphorylation has been reported to enhance its interactions with the ATR and the 9-1-1 checkpoint clamp (66,67). Hence, although further investigations are necessary to address the link between RPA2 phosphorylation and CTF18-RPA interaction, my present findings could shed light on the molecular basis of the initiation of replication stress response in mammalian cells.

Since CTF18 appears to directly activate Pol ϵ enzymatic activities and potentially load mono-ubiquitylated PCNA for Polymerase switching, it may be important for translesion DNA synthesis. It has been reported that some clamp loaders, such as RFC1, Rad17, and small subunits RFC2-4 but not CTF18 accumulate in the chromatin fraction in response to methyl methane sulfonate (MMS) and UV-irradiation, which cause replication fork stalling (68). Given no evidence for the regulation of CTF18 in response to DNA damages, it is unclear how CTF18 contribute to TLS. In this study, we focus on the RPA-CTF18 interaction in chromatin by cytoskeleton treatment and found that the interaction occurs in chromatin in response to UV-irradiation during S-phase by performing *in situ* Proximity Ligation Assay (PLA). Furthermore, ssDNA pull-down assay reveals that CTF18 could interact with RPA-ssDNA complex, which corresponds to the behavior of E3 ubiquitin ligase Rad18 (49). Taken together, my findings suggest

that CTF18 as well as Rad18 is involved in TLS via interaction with RPA complex as scaffold in response to UV-irradiation.

Among the four clamp loader complexes, the Elg1-RFC is thought to act principally as an unloader for PCNA from nascent DNA after the passage of replication forks and thereby regulate PCNA levels in chromatin (69-71). Meanwhile, Bylund and Burgers demonstrated that CTF18-RFC also unloads PCNA specifically when ssDNA is coated with RPA, and they proposed a model in which this unloading activity of CTF18-RFC may contribute to establishing sister chromatid cohesion (72). However, considering my present result that CTF18 binds to RPA after UV-irradiation during S phase, it is possible that CTF18-RFC may remove monoubiquitinated PCNA after replicative bypass of UV-induced CPD with Pol η and subsequently reload unmodified PCNA to restart normal DNA replication. Thus, our findings will provide insight into the mechanism how DNA polymerases switch during translesion DNA synthesis.

My results show that CTF18 interacts with not only RPA complex but also ssDNA in RPA dependent manner. In addition, follow-up observation of PLA signals shows that CTF18-RPA complex after UV-irradiation transiently increase and then gradually decrease, considering that this time-dependent change appears to correspond to S-phase checkpoint response mediated by ATR-CHK1 pathway. Recent studies with budding yeast have established that CTF18 mediates activation of S-phase checkpoint depending on the association with DNA polymerase epsilon (59). In fact, depletion of CTF18 decreases the Mec1 (ATR in human) dependent phosphorylation and displays the sensitivity to HU. Because RPA-ssDNA complex is a platform for checkpoint signaling,

the interaction between CTF18 and RPA may act as the trigger for CHK1-ATR signaling and be required for its association with DNA polymerase and other proteins.

In conclusion, here I present the interaction between CTF18 and RPA complex as a novel regulation of CTF18 in response to DNA damage. This molecular interaction highlights the function of CTF18 as alternative clamp loader for genome integrity and may provide an important clue for elucidating regulation of CTF18 in s-phase checkpoint signal and translesion DNA synthesis.

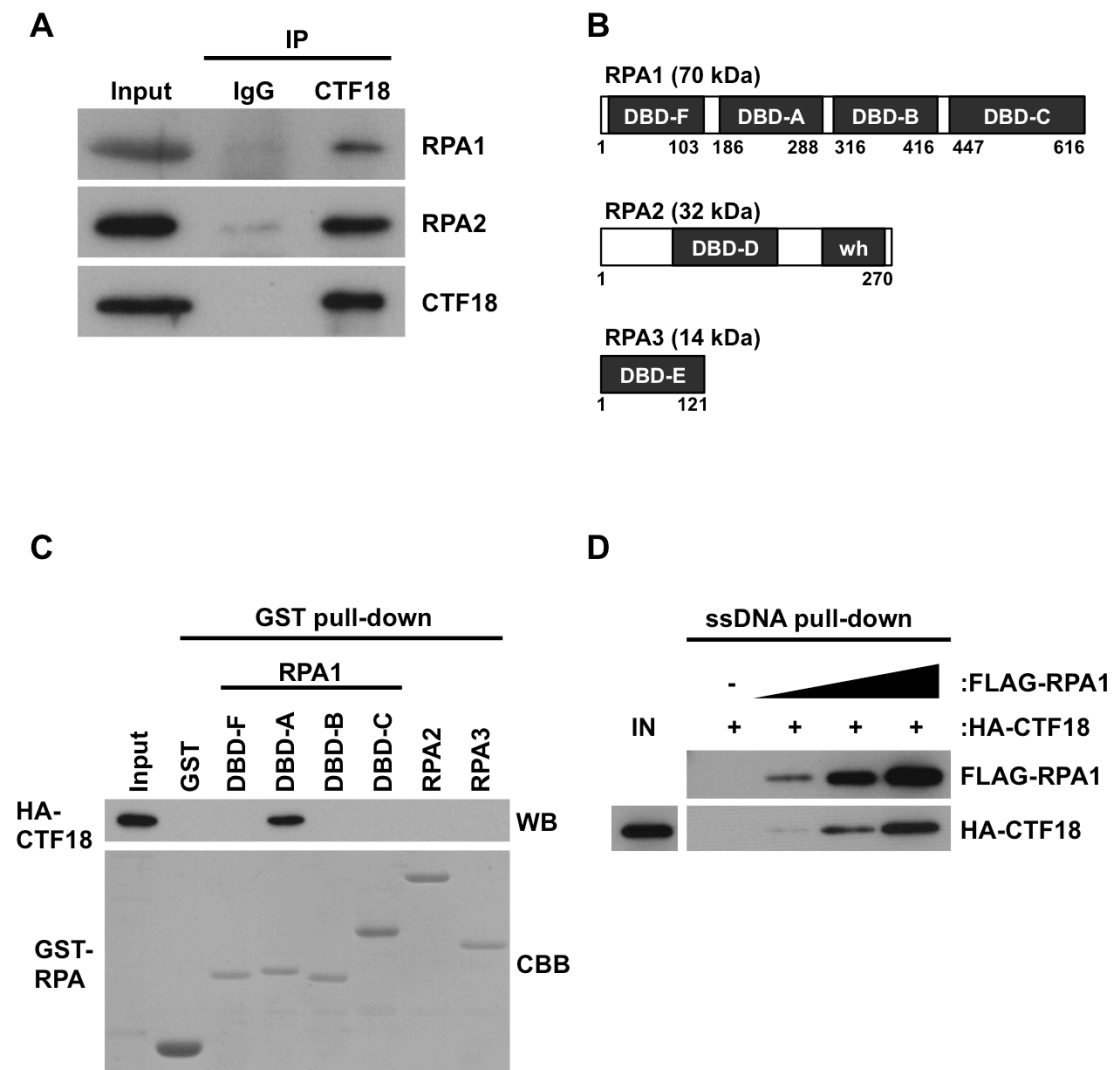


Figure III-1 CTF18 interacts with RPA complex in vivo and in vitro

(A) Endogenous CTF18 interacts with RPA1 and RPA2. Whole-cell lysates from HEK293 cells were immunoprecipitated with normal IgG or anti-CTF18 antibody, followed by Western blotting with antibodies as indicated. (B) Schematic representation of RPA1, 2 and 3. DBD, DNA-binding domain. wh, wing helix domain. (C) DBD-A domain of RPA1 is required for CTF18 binding. In vitro translated HA-CTF18 was incubated with GST, GST-RPA1 fragment, RPA2 and RPA3, followed by Western blotting with anti-HA antibody. GST proteins are shown by CBB staining. (D) CTF18 is recruited to ssDNA in a manner dependent on RPA1. ssDNA-conjugated beads were preincubated with increasing amounts of FLAG-RPA1, and then incubated with whole-cell lysates from HEK293T cells expressing HA-CTF18, followed by Western blotting with indicated antibodies.

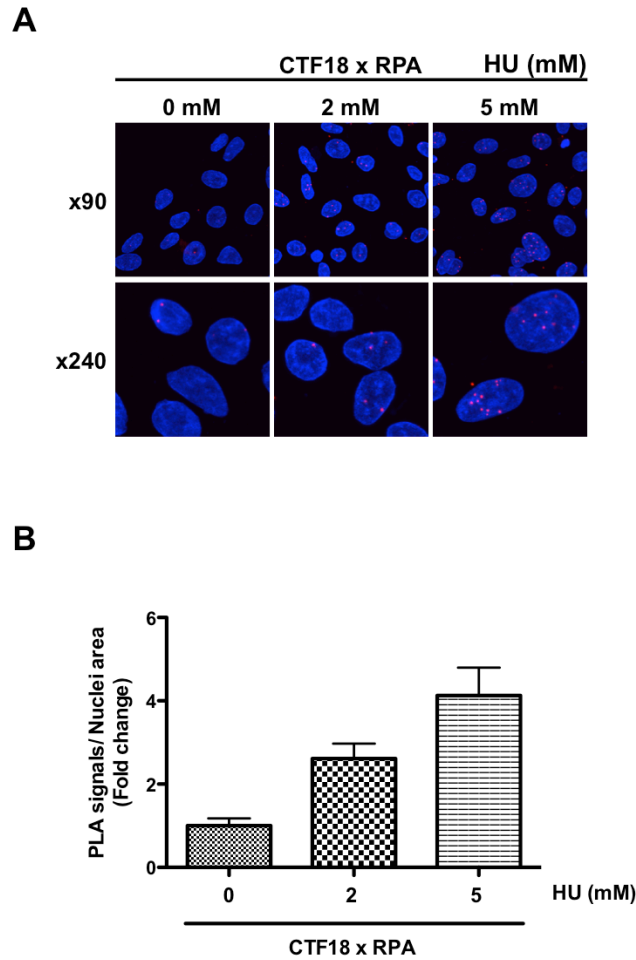
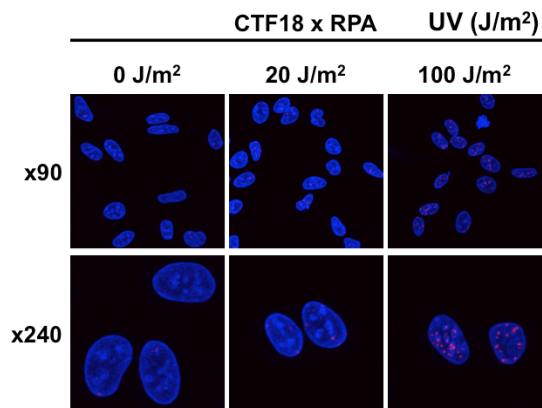
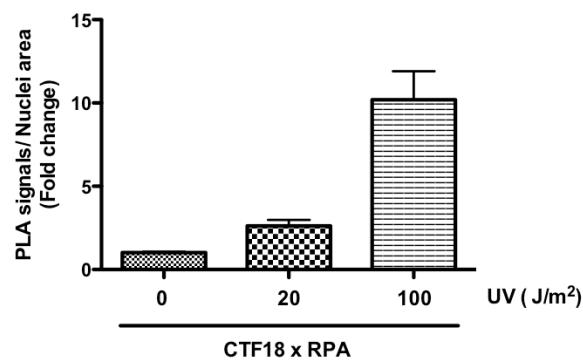


Figure III-2 CTF18 is associated with RPA in presence of replication stress

(A) The interaction between CTF18 and RPA complex occurs after treatment of hydroxyurea. HEK293 cells were synchronized to S phase by double thymidine block and then treated with the indicated concentration of hydroxyurea. After 2 hours, cells were treated with CSK/Triton buffer followed by fixation, and then *in situ* proximity ligation assay (PLA) was performed with anti-RPA2 and anti-CTF18 antibodies. The red fluorescence foci indicate the proximity of the two proteins (magnification, x90 or x240). (B) Quantification of PLA signals in (A) using Duolink Image Tool. Duolink Image Tool was used to quantify PLA signals (n=3, x90 magnification). The vertical axis shows the total nuclear PLA signals divided by nuclei area and normalized to non-treatment group, and the horizontal axis indicates the concentration of HU. Error bars indicate \pm SEM of three different fields.

A**B****Figure III-3 CTF18 interacts with RPA after UV-irradiation**

(A) The CTF18-RPA interaction occurs after exposure to UV irradiation. HEK293 cells were synchronized to S phase by double thymidine block and then irradiated with indicated dose of UV light. The PLA was performed as shown in Figure II. (B) Quantification of PLA signals in (A) using Duolink Image Tool.

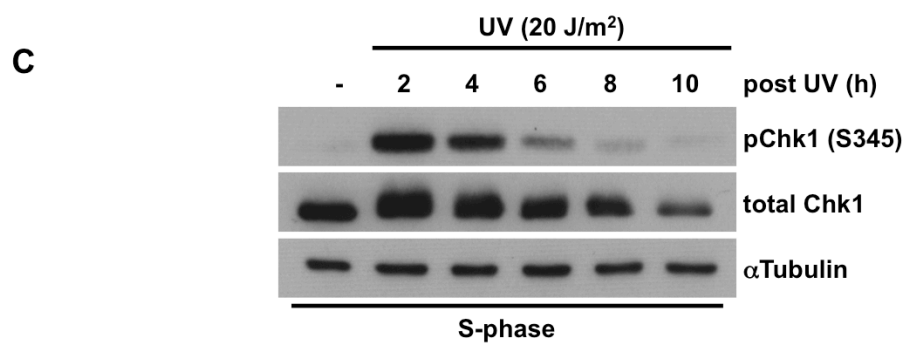
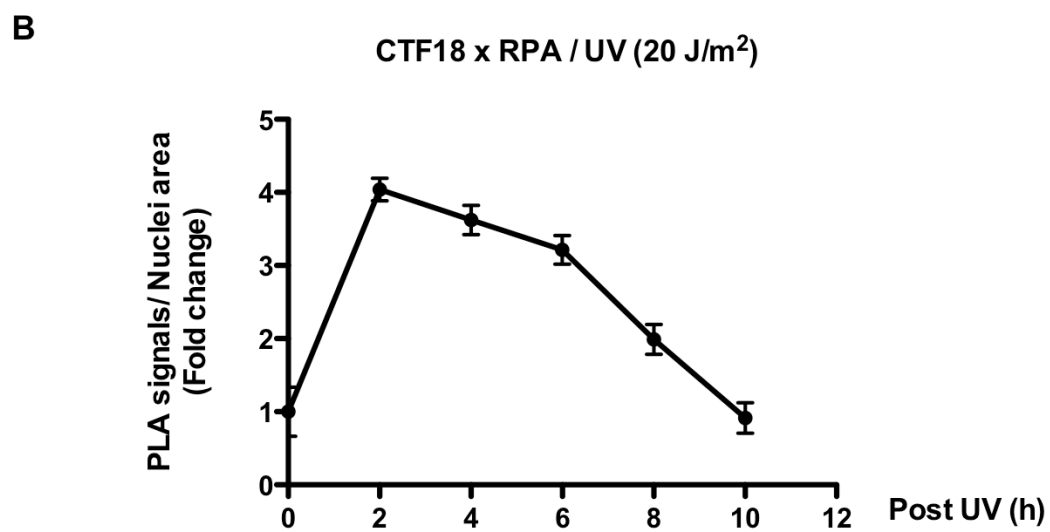
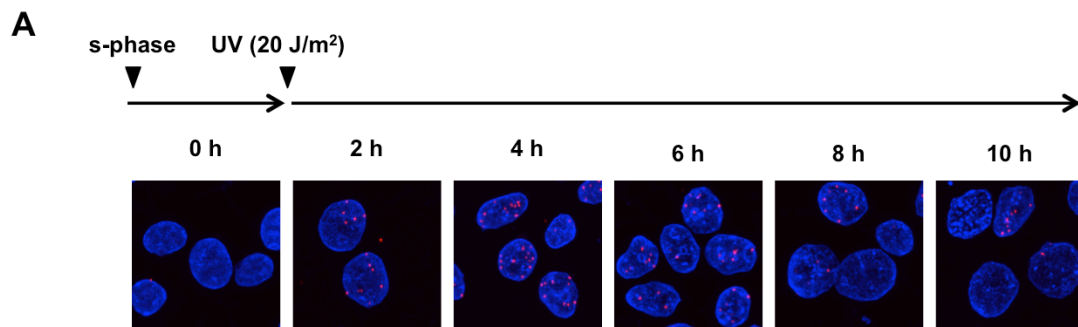


Figure III-4 UV-induced CTF18-RPA interaction and Chk1 phosphorylation gradually decrease with time

(A) The dissociation kinetics of CTF18-RPA complex in HEK293 cells. PLA were performed with indicated time course (magnification, x240). (B) Duolink Image Tool was used to quantify PLA signals. The vertical axis shows the total nuclear PLA signals divided by nuclei area and normalized to non-irradiation group, and the horizontal axis indicates the time course after UV irradiation. Error bars indicate \pm SEM of three different fields. (C) The phosphorylation of Chk1 decreases after UV irradiation. HEK293 cells synchronized at S phase were irradiated with UV (20 J/m²). After indicated time, whole-cell lysates were immunoblotted with antibodies as indicated.

Chapter IV

Concluding Remarks

Accumulating evidence indicated that transcriptional factor FOXO/DAF-16 plays an important role in multiple higher biological processes, such as anti-aging, tumor suppression and embryonic development. To this date, many studies have revealed a variety of FOXO target genes, while their finding could not elucidate the molecular mechanism underlying the higher biological processes regulated by FOXO. In chapter II, because of close relationships between DNA damage response and such biological process, I focus on involvement of FOXO1/DAF-16 in DNA damage response and present evidence that FOXO1/DAF-16 contributes to UV-induced DNA damage tolerance independently of its transcriptional activity in mammalian cells and *C. elegans*. Interestingly, it appears that its function requires for the interaction between FOXO and RPA that play an essential role in DNA metabolism. In chapter III, to get deep insight into regulation of clamp loader CTF18 in replication stress response, I investigated the interaction between RPA and CTF18. *In situ* Proximity ligation assay (*in situ* PLA) clearly reveals that their interaction increase in chromatin after exposure to replication stresses. Given the function as scaffold for a variety of proteins, such as DNA helicase, signal transducer and chromatin remodeler, in DNA damage response, the replication stress-dependent interaction between RPA and CTF18 is appears to be the critical step in regulation of CTF18 in replication stress response. Both of these studies show the importance of RPA in DNA damage response during s-phase. Recently, I found that

FOXO1 interacted with RPA interactants related replication stress responses, so that these results imply the possibility that FOXO1 contributes to, in addition to translesion DNA synthesis, other responses in which RPA is involved. Considering the correlation between disruption of replication stress response and the biological processes, such as ageing, development abnormality and cancer, further studies would be expected to elucidate the relationship between a function of the transactivation-independent FOXO1/DAF-16 in DNA damage tolerance and such biological processes.

Acknowledgments

I would like to express my deep gratitude to all those who provided me guidance, support and encouragement during the preparation of this dissertation. Most of all, I would like to express my sincere thanks to Professor Akiyoshi Fukamizu for all his support and guidance throughout my research work. I am deeply indebted to Dr. Hiroaki Daitoku, Professor Keiji Tanimoto, Dr. Koichiro Kako, Dr. Junji Ishida and Dr. Keiko Hirota for their teaching about the helpful discussions or experimental techniques. In addition, I would like to give my thanks all members of Fukamizu Laboratory for their kind support. Finally, I appreciate greatly the helps of my parents and friends.

References

1. Papamichos-Chronakis, M., and Peterson, C. L. (2013) Chromatin and the genome integrity network. *Nat Rev Genet* **14**, 62-75
2. Lopez-Otin, C., Blasco, M. A., Partridge, L., Serrano, M., and Kroemer, G. (2013) The hallmarks of aging. *Cell* **153**, 1194-1217
3. Eijkelenboom, A., and Burgering, B. M. (2013) FOXOs: signalling integrators for homeostasis maintenance. *Nature reviews. Molecular cell biology* **14**, 83-97
4. Calnan, D. R., and Brunet, A. (2008) The FoxO code. *Oncogene* **27**, 2276-2288
5. Xie, Q., Chen, J., and Yuan, Z. (2012) Post-translational regulation of FOXO. *Acta biochimica et biophysica Sinica* **44**, 897-901
6. Brunet, A., Bonni, A., Zigmond, M. J., Lin, M. Z., Juo, P., Hu, L. S., Anderson, M. J., Arden, K. C., Blenis, J., and Greenberg, M. E. (1999) Akt promotes cell survival by phosphorylating and inhibiting a Forkhead transcription factor. *Cell* **96**, 857-868
7. Kenyon, C., Chang, J., Gensch, E., Rudner, A., and Tabtiang, R. (1993) A *C. elegans* mutant that lives twice as long as wild type. *Nature* **366**, 461-464
8. Daitoku, H., Hatta, M., Matsuzaki, H., Aratani, S., Ohshima, T., Miyagishi, M., Nakajima, T., and Fukamizu, A. (2004) Silent information regulator 2 potentiates Foxo1-mediated transcription through its deacetylase activity. *Proc Natl Acad Sci U S A* **101**, 10042-10047
9. Yamagata, K., Daitoku, H., Takahashi, Y., Namiki, K., Hisatake, K., Kako, K., Mukai, H., Kasuya, Y., and Fukamizu, A. (2008) Arginine methylation of FOXO transcription factors inhibits their phosphorylation by Akt. *Mol Cell* **32**, 221-231
10. Tang, E. D., Nunez, G., Barr, F. G., and Guan, K. L. (1999) Negative Regulation of the Forkhead Transcription Factor FKHR by Akt. *Journal of Biological Chemistry* **274**, 16741-16746
11. Altieri, F., Grillo, C., Maceroni, M., and Chichiarelli, S. (2008) DNA damage and repair: from molecular mechanisms to health implications. *Antioxid Redox Signal* **10**, 891-937

12. Yang, W. (2014) An overview of Y-Family DNA polymerases and a case study of human DNA polymerase η . *Biochemistry* **53**, 2793-2803
13. Huttner, D., and Ulrich, H. D. (2014) Cooperation of replication Protein A with the ubiquitin ligase Rad18 in DNA damage bypass. *Cell Cycle* **7**, 3629-3633
14. Haracska, L., Johnson, R. E., Unk, I., Phillips, B., Hurwitz, J., Prakash, L., and Prakash, S. (2001) Physical and functional interactions of human DNA polymerase η with PCNA. *Molecular and cellular biology* **21**, 7199-7206
15. Shiomi, Y., Masutani, C., Hanaoka, F., Kimura, H., and Tsurimoto, T. (2007) A second proliferating cell nuclear antigen loader complex, Ctf18-replication factor C, stimulates DNA polymerase η activity. *J Biol Chem* **282**, 20906-20914
16. Huttner, D., and Ulrich, H. D. (2008) Cooperation of replication Protein A with the ubiquitin ligase Rad18 in DNA damage bypass. *Cell Cycle* **7**, 3629-3633
17. Fu, Y., Zhu, Y., Zhang, K., Yeung, M., Durocher, D., and Xiao, W. (2008) Rad6-Rad18 mediates a eukaryotic SOS response by ubiquitinating the 9-1-1 checkpoint clamp. *Cell* **133**, 601-611
18. Dominguez-Sola, D., Ying, C. Y., Grandori, C., Ruggiero, L., Chen, B., Li, M., Galloway, D. A., Gu, W., Gautier, J., and Dalla-Favera, R. (2007) Non-transcriptional control of DNA replication by c-Myc. *Nature* **448**, 445-451
19. Choi, J. H., Lindsey-Boltz, L. A., Kemp, M., Mason, A. C., Wold, M. S., and Sancar, A. (2010) Reconstitution of RPA-covered single-stranded DNA-activated ATR-Chk1 signaling. *Proc Natl Acad Sci U S A* **107**, 13660-13665
20. Bomgarden, R. D., Lupardus, P. J., Soni, D. V., Yee, M. C., Ford, J. M., and Cimprich, K. A. (2006) Opposing effects of the UV lesion repair protein XPA and UV bypass polymerase η on ATR checkpoint signaling. *The EMBO journal* **25**, 2605-2614
21. Tsai, W. B., Chung, Y. M., Takahashi, Y., Xu, Z., and Hu, M. C. (2008) Functional interaction between FOXO3a and ATM regulates DNA damage response. *Nature cell biology* **10**, 460-467
22. Watanabe, K., Tateishi, S., Kawasuji, M., Tsurimoto, T., Inoue, H., and Yamaizumi, M. (2004) Rad18 guides pol η to replication stalling sites through

- physical interaction and PCNA monoubiquitination. *The EMBO journal* **23**, 3886-3896
23. Marechal, A., and Zou, L. (2015) RPA-coated single-stranded DNA as a platform for post-translational modifications in the DNA damage response. *Cell Res* **25**, 9-23
 24. Hirota, K., Sakamaki, J., Ishida, J., Shimamoto, Y., Nishihara, S., Kodama, N., Ohta, K., Yamamoto, M., Tanimoto, K., and Fukamizu, A. (2008) A combination of HNF-4 and Foxo1 is required for reciprocal transcriptional regulation of glucokinase and glucose-6-phosphatase genes in response to fasting and feeding. *The Journal of biological chemistry* **283**, 32432-32441
 25. Lapierre, L. R., and Hansen, M. (2012) Lessons from *C. elegans*: signaling pathways for longevity. *Trends in endocrinology and metabolism: TEM* **23**, 637-644
 26. Henderson, S. T., and Johnson, T. E. (2001) daf-16 integrates developmental and environmental inputs to mediate aging in the nematode *Caenorhabditis elegans*. *Current biology : CB* **11**, 1975-1980
 27. Lans, H., Marteijn, J. A., Schumacher, B., Hoeijmakers, J. H., Jansen, G., and Vermeulen, W. (2010) Involvement of global genome repair, transcription coupled repair, and chromatin remodeling in UV DNA damage response changes during development. *PLoS genetics* **6**, e1000941
 28. Wang, F., Marshall, C. B., Li, G. Y., Yamamoto, K., Mak, T. W., and Ikura, M. (2009) Synergistic Interplay between Promoter Recognition and CBP/p300 Coactivator Recruitment by FOXO3a. *Acs Chem Biol* **4**, 1017-1027
 29. Falbo, K. B., Alabert, C., Katou, Y., Wu, S., Han, J., Wehr, T., Xiao, J., He, X., Zhang, Z., Shi, Y., Shirahige, K., Pasero, P., and Shen, X. (2009) Involvement of a chromatin remodeling complex in damage tolerance during DNA replication. *Nature structural & molecular biology* **16**, 1167-1172
 30. Niimi, A., Chambers, A. L., Downs, J. A., and Lehmann, A. R. (2012) A role for chromatin remodellers in replication of damaged DNA. *Nucleic acids research* **40**, 7393-7403
 31. Riedel, C. G., Downen, R. H., Lourenco, G. F., Kirienko, N. V., Heimbucher, T., West, J. A., Bowman, S. K., Kingston, R. E., Dillin, A., Asara, J. M., and

- Ruvkun, G. (2013) DAF-16 employs the chromatin remodeller SWI/SNF to promote stress resistance and longevity. *Nat Cell Biol* **15**, 491-501
32. Hatta, M., and Cirillo, L. A. (2007) Chromatin opening and stable perturbation of core histone:DNA contacts by FoxO1. *The Journal of biological chemistry* **282**, 35583-35593
 33. Fujimoto, M., Takaki, E., Takii, R., Tan, K., Prakasam, R., Hayashida, N., Iemura, S., Natsume, T., and Nakai, A. (2012) RPA assists HSF1 access to nucleosomal DNA by recruiting histone chaperone FACT. *Mol Cell* **48**, 182-194
 34. Daitoku, H., Sakamaki, J., and Fukamizu, A. (2011) Regulation of FoxO transcription factors by acetylation and protein-protein interactions. *Biochimica et biophysica acta* **1813**, 1954-1960
 35. Sakamaki, J., Daitoku, H., Yoshimochi, K., Miwa, M., and Fukamizu, A. (2009) Regulation of FOXO1-mediated transcription and cell proliferation by PARP-1. *Biochem Biophys Res Commun* **382**, 497-502
 36. Tallis, M., Morra, R., Barkauskaite, E., and Ahel, I. (2014) Poly(ADP-ribosylation) in regulation of chromatin structure and the DNA damage response. *Chromosoma* **123**, 79-90
 37. Nicolae, C. M., Aho, E. R., Vlahos, A. H., Choe, K. N., De, S., Karras, G. I., and Moldovan, G. L. (2014) The ADP-ribosyltransferase PARP10/ARTD10 interacts with proliferating cell nuclear antigen (PCNA) and is required for DNA damage tolerance. *J Biol Chem* **289**, 13627-13637
 38. Barlow, C., Hirotsune, S., Paylor, R., Liyanage, M., Eckhaus, M., Collins, F., Shiloh, Y., Crawley, J. N., Ried, T., Tagle, D., and Wynshaw-Boris, A. (1996) Atm-deficient mice: a paradigm of ataxia telangiectasia. *Cell* **86**, 159-171
 39. Brown, E. J., and Baltimore, D. (2000) ATR disruption leads to chromosomal fragmentation and early embryonic lethality. *Genes & development* **14**, 397-402
 40. Hosaka, T., Biggs, W. H., 3rd, Tieu, D., Boyer, A. D., Varki, N. M., Cavenee, W. K., and Arden, K. C. (2004) Disruption of forkhead transcription factor (FOXO) family members in mice reveals their functional diversification. *Proceedings of the National Academy of Sciences of the United States of America* **101**, 2975-2980

41. Lin, Q., Clark, A. B., McCulloch, S. D., Yuan, T., Bronson, R. T., Kunkel, T. A., and Kucherlapati, R. (2006) Increased susceptibility to UV-induced skin carcinogenesis in polymerase eta-deficient mice. *Cancer research* **66**, 87-94
42. Mueller, M. M., Castells-Roca, L., Babu, V., Ermolaeva, M. A., Muller, R. U., Frommolt, P., Williams, A. B., Greiss, S., Schneider, J. I., Benzing, T., Schermer, B., and Schumacher, B. (2014) DAF-16/FOXO and EGL-27/GATA promote developmental growth in response to persistent somatic DNA damage. *Nat Cell Biol* **16**, 1168-1179
43. Ro, S. H., Liu, D., Yeo, H., and Paik, J. H. (2013) FoxOs in neural stem cell fate decision. *Archives of biochemistry and biophysics* **534**, 55-63
44. Tothova, Z., and Gilliland, D. G. (2007) FoxO transcription factors and stem cell homeostasis: insights from the hematopoietic system. *Cell stem cell* **1**, 140-152
45. Brnzei, D., and Foiani, M. (2008) Regulation of DNA repair throughout the cell cycle. *Nat Rev Mol Cell Biol* **9**, 297-308
46. Cimprich, M. K. Z. a. K. A. (2014) Causes and consequences of replication stress. *NATURE CELL BIOLOGY* **16**, 2-9
47. Zou, L., and Elledge, S. J. (2003) Sensing DNA damage through ATRIP recognition of RPA-ssDNA complexes. *Science* **300**, 1542-1548
48. Smits, V. A., and Gillespie, D. A. (2015) DNA damage control: regulation and functions of checkpoint kinase 1. *FEBS J* **282**, 3681-3692
49. Davies, A. A., Huttner, D., Daigaku, Y., Chen, S., and Ulrich, H. D. (2008) Activation of ubiquitin-dependent DNA damage bypass is mediated by replication protein a. *Mol Cell* **29**, 625-636
50. Despras, E., Daboussi, F., Hyrien, O., Marheineke, K., and Kannouche, P. L. (2010) ATR/Chk1 pathway is essential for resumption of DNA synthesis and cell survival in UV-irradiated XP variant cells. *Hum Mol Genet* **19**, 1690-1701
51. Garcia-Rodriguez, L. J., De Piccoli, G., Marchesi, V., Jones, R. C., Edmondson, R. D., and Labib, K. (2015) A conserved Pol binding module in Ctf18-RFC is required for S-phase checkpoint activation downstream of Mec1. *Nucleic Acids Res* **43**, 8830-8838
52. Crabbe, L., Thomas, A., Pantesco, V., De Vos, J., Pasero, P., and Lengronne, A. (2010) Analysis of replication profiles reveals key role of RFC-Ctf18 in yeast replication stress response. *Nat Struct Mol Biol* **17**, 1391-1397

53. Takashi Kubota, S.-i. H., Kayo Yamada, Angus I. Lamond,, and Donaldson, a. A. D. (2011) Quantitative Proteomic Analysis of Chromatin Reveals that Ctf18 Acts in the DNA Replication Checkpoint. *Molecular & Cellular Proteomics* **10**
54. Laure Crabbé, A. T., Véronique Pantesco, John De Vos2, Philippe Pasero, & Armelle Lengronne. (2010) Analysis of replication profiles reveals key role of RFC-Ctf18 in yeast replication stress response. *nature structural & molecular biology* **17** 1391- 1398
55. Mailand, N., Gibbs-Seymour, I., and Bekker-Jensen, S. (2013) Regulation of PCNA-protein interactions for genome stability. *Nat Rev Mol Cell Biol* **14**, 269-282
56. Kanellis, P., Agyei, R., and Durocher, D. (2003) Elg1 Forms an Alternative PCNA-Interacting RFC Complex Required to Maintain Genome Stability. *Current Biology* **13**, 1583-1595
57. Mohammed Bellaoui, M. C., Jiongwen Ou, Hong Xu, Charles Boone and Grant W. Brown. (2003) Elg1 forms an alternative RFC complex important for DNA replication and genome integrity. *The EMBO Journal* **22**
58. Parrilla-Castellar, E. R., Arlander, S. J., and Karnitz, L. (2004) Dial 9-1-1 for DNA damage: the Rad9-Hus1-Rad1 (9-1-1) clamp complex. *DNA Repair (Amst)* **3**, 1009-1014
59. Luis J. Garc'ia-Rodr'iguez, G. D. P., Vanessa Marchesi, Richard C. Jones,, and Labib, R. D. E. a. K. (2015) A conserved Pole binding module in Ctf18-RFC is required for S-phase checkpoint activation downstream of Mec1. *Nucleic Acids Res.* **43**, 8830-8838
60. Taniguchi, T., Garcia-Higuera, I., Andreassen, P. R., Gregory, R. C., Grompe, M., and D'Andrea, A. D. (2002) S-phase-specific interaction of the Fanconi anemia protein, FANCD2, with BRCA1 and RAD51. *Blood* **100**, 2414-2420
61. Vassin, V. M., Anantha, R. W., Sokolova, E., Kanner, S., and Borowiec, J. A. (2009) Human RPA phosphorylation by ATR stimulates DNA synthesis and prevents ssDNA accumulation during DNA-replication stress. *J Cell Sci* **122**, 4070-4080
62. Liaw, H., Lee, D., and Myung, K. (2011) DNA-PK-dependent RPA2 hyperphosphorylation facilitates DNA repair and suppresses sister chromatid exchange. *PLoS One* **6**, e21424

63. Liu, S., Opiyo, S. O., Manthey, K., Glanzer, J. G., Ashley, A. K., Amerin, C., Troksa, K., Shrivastav, M., Nickoloff, J. A., and Oakley, G. G. (2012) Distinct roles for DNA-PK, ATM and ATR in RPA phosphorylation and checkpoint activation in response to replication stress. *Nucleic Acids Res* **40**, 10780-10794
64. Olson, E., Nievera, C. J., Klimovich, V., Fanning, E., and Wu, X. (2006) RPA2 is a direct downstream target for ATR to regulate the S-phase checkpoint. *J Biol Chem* **281**, 39517-39533
65. Vassin, V. M., Wold, M. S., and Borowiec, J. A. (2004) Replication Protein A (RPA) Phosphorylation Prevents RPA Association with Replication Centers. *Molecular and Cellular Biology* **24**, 1930-1943
66. Wu, X., Shell, S. M., and Zou, Y. (2005) Interaction and colocalization of Rad9/Rad1/Hus1 checkpoint complex with replication protein A in human cells. *Oncogene* **24**, 4728-4735
67. Wu, X., Yang, Z., Liu, Y., and Zou, Y. (2005) Preferential localization of hyperphosphorylated replication protein A to double-strand break repair and checkpoint complexes upon DNA damage. *Biochem J* **391**, 473-480
68. Tomida, J., Masuda, Y., Hiroaki, H., Ishikawa, T., Song, I., Tsurimoto, T., Tateishi, S., Shiomi, T., Kamei, Y., Kim, J., Kamiya, K., Vaziri, C., Ohmori, H., and Todo, T. (2008) DNA damage-induced ubiquitylation of RFC2 subunit of replication factor C complex. *J Biol Chem* **283**, 9071-9079
69. Kubota, T., Nishimura, K., Kanemaki, M. T., and Donaldson, A. D. (2013) The Elg1 replication factor C-like complex functions in PCNA unloading during DNA replication. *Mol Cell* **50**, 273-280
70. Lee, K. Y., Fu, H., Aladjem, M. I., and Myung, K. (2013) ATAD5 regulates the lifespan of DNA replication factories by modulating PCNA level on the chromatin. *J Cell Biol* **200**, 31-44
71. Ulrich, H. D. (2013) New insights into replication clamp unloading. *J Mol Biol* **425**, 4727-4732
72. Bylund G. O. and Burgers, P. M. (2005) Replication protein A-directed unloading of PCNA by the Ctf18 cohesion establishment complex. *Mol Cell Biol* **25**, 5445-5455